FACTORS CONTROLLING THE FRACTURE TOUGHNESS OF CRYOGENIC ALLOYS

Wade Alan Horwood
(M. S. thesis)

December 1972

Prepared for the U. S. Atomic Energy Commission
under Contract W-7405-ENG-48

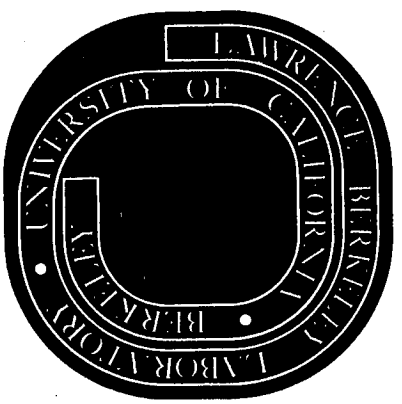

LBL-1121
c.1

DISCLAIMER

FACTORS CONTROLLING THE FRACTURE TOUGHNESS OF CRYOGENIC ALLOYS

Contents

FACTORS CONTROLLING THE FRACTURE TOUGHNESS OF CRYOGENIC ALLOYS

Wade Alan Horwood

Inorganic Materials Research Division, Lawrence Berkeley Laboratory and Department of Materials Science and Engineering, College of Engineering; University of California, Berkeley, California

ABSTRACT

This study was initiated to attempt to design, using a basic knowledge of materials and processing, an Fe base BCC alloy having superior combinations of strength and toughness at -196°C. An alloy of Fe-12 wt% Ni-0.5 wt% Ti was chosen for the investigation.

The optimum properties of this alloy at room temperature and at -196°C are given below:

	23°C	-196°C
Charpy V-notch energy	220 ft-lb	130-150 ft-lb
0.2% yield stress (ksi)	90-98	135-150
Tensile stress (ksi)	95-110	150-165
% Elongation in 1 inch	22%	22%
% Reduction in area	85%	75%

These unusual mechanical properties are attainable with several different heat treatments. Structural studies reveal that the impact properties are highly dependent on the grain size.

The alloy shows much promise as a high strength, high toughness alloy for low temperature use, exhibiting combinations of strength and toughness unmatched by available commercial cryogenic alloys.

I. INTRODUCTION

With the rapidly expanding use of liquified gas products for scientific and industrial applications, there is an urgent need for materials which are both strong and tough at temperatures to -200°C and below. Unfortunately, mechanical properties can change drastically with temperature, and a material which is ductile at room temperature can become extremely brittle, and therefore unsafe for structural purposes, when operating temperatures are lowered by as little as 50 to 100°C.

The most common metals have either the FCC or BCC lattice structure and these two structures are different in their response to change in temperature. The FCC is characterized by an increase in tensile strength with decreasing temperature, while the yield strength and impact resistance are in general relatively temperature insensitive.[1] The yield strength is normally low. The behavior of BCC materials is quite dissimilar. With decreasing temperature, the tensile strength, in most cases, changes relatively little while the yield strength increases rapidly.[1,2] The impact resistance shows a sharp transition from high to low resistance to brittle fracture. This drastic change in impact resistance of BCC materials occurs in a narrow temperature range and is called the Nil Ductility Transition (NDT).

Currently, two of the most commonly used cryogenic alloys are type 304 L stainless steel (FCC) and the 9% Ni, 0.1% C steel (BCC).[3,4] Two of the most important mechanical properties required for low temperature service are yield strength and resistance to brittle fracture. These

properties are tabulated below[1,4,5,6,7,8] for the 9% Ni steel and 304 L stainless steel at a temperature of -196°C.

	Yield Strength	Charpy V-Notch
9% Ni Steel	140,000 psi	60 to 80 ft-lb
304 L SS	60,000 psi	120 to 170 ft-lb

It is obvious that these two materials do not have optimum combinations of strength and toughness. The 304 L stainless steel has very high resistance to brittle fracture as indicated by the standard Charpy V-notch energy. However, it has a low yield strength. The 9% Ni steel has a high yield strength but a much lower Charpy impact value. Thus, both materials are less than ideal i.e., one combining both high strength and high toughness.

Other than the work of Brophy and Miller[9] describing the unusually good low temperature impact properties of the 8-10% Ni steels containing 0.1%C, little has been done to develop new BCC alloys. New heat treatments have been developed for the 9% Ni steels to improve their low temperature toughness[5,10] and studies have been made of lower nickel content steels[3,11] but no new alloys with superior low temperature properties have appeared for several decades.

As discussed above, the materials presently in existance for low temperature service show either high strength and relatively low

toughness or high toughness and low strength. This type of trade off has, in the past, been taken as a fact of life, and attempts to use a basic knowledge of materials to acquire, simultaneously, increased strength and improved toughness, have been few.

A variety of metallurgical phenomena need to be considered in the development of an α-Fe cryogenic alloy. The major factors that influenced the composition used in this study and its resultant processing were: the effects of substitutional and interstitial elements, control of grain size, precipitates and dislocation substructure.

Interstitials, especially carbon, are known to cause rapid embrittlement of α-Fe at low temperatures.[2,12,13,14] The mechanism is probably that of segregation at dislocations; thereby inhibiting dislocation motion i.e., plastic deformation.[1] To combat these deliterious effects, interstitial element concentrations must be kept as low as possible, either by removal during manufacture or by alloy chemistry; such as the introduction of a strong getter to precipitate them as finely dispersed, innocous particles.

Reduction of the grain size is a form of microstructural control by which low temperature properties can be improved. A strength increase accompanies grain size reduction, and Smith[14] and Hodge[15] have demonstrated the relationship between grain size, Nil Ductility Transition (NDT) temperature and tensile ductility. This increased ductility is believed to be due to the accompaning large increase in the difference between the yield stress and the fracture stress,[16]

which allows greater plastic deformation and energy absorption before fracture. It is known that the grain size can be refined by alloy additions, hot or cold deformation and/or phase transformations.

Precipitates, although effective in increasing the yield stress, are normally detrimental to low temperature ductility. However, small, finely dispersed, noncoherent precipitates can improve both strength and ductility by decreasing the length of stable dislocation arrays.[16] This is essentially a way of decreasing the effective grain size of the material and should therefore improve the notch toughness.

Several substitutional elements are known to lower the NDT temperature and to improve the low temperature ductility and the impact resistance of α-Fe. The most suitable of these as a major alloying addition is nickel.[3,12,13,17] Although the reason is not well understood, nickel is unique in its ability to profoundly improve the low temperature ductility of α-Fe.[9,17] Elements other than nickel improve ductility by affecting the distribution and morphology of carbides[12] or removing interstitials by precipitation.

Dislocation substructure plays a large part in low temperature toughness. Ideally, a substructure containing large numbers of lightly pinned, mobile dislocations, intimately mixed with areas almost devoid of dislocations would produce good low temperature properties. The highly dislocated areas would provide strength, while the areas containing few dislocations would provide an opportunity for relieving high stresses by providing dislocation free areas for the movement of mobile dislocations.

Given the above considerations, the desirable features of a low temperature BCC alloy are fine grain size, low interstitial content (plus a getter to remove those present from undesirable sites), moderate nickel additions (to improve properties without making the alloy too expensive), a duplex substructure, and the presence (for strengthening) of noncoherent precipitates. The Fe-Ni-Ti system meets all these requirements. By varying composition and heat treatment, a wide variety of strength levels, microstructures and substructures can be easily obtained. The system has an α to γ phase transformation temperature which decreases with increasing nickel content. Thus it is possible both to decrease grain size by a phase transformation at relatively low heat treating temperatures and to attain the low temperature ductility normally associated with nickel containing alloys. Precipitation of ductile Ni_3Ti particles as a finely dispersed second phase is possible in this system by simple α heat treatment, and in addition, the titanium acts as a strong getter to remove carbon and other tramp elements from solution in the matrix. The duplex dislocation substructure produced on cooling through the $\gamma \rightarrow \alpha$ phase transformation is similar to that described as highly desirable earlier in the introduction.[18]

II. EXPERIMENTAL PROCEDURE

A. Material Preparation

The alloy used for this investigation was made by induction melting in an argon atmosphere from high purity Fe, Ni and Ti. The chemical analysis of the three 20 lb ingots used are given in Table 1. The as-cast ingots were homogenized for 50 hrs at 1100°C, air cooled, and forged at 1100°C to 5/8 in. dia rod and air cooled.

B. Heat Treatment

Three inch long sections of as forged rod were heat treated in an air furnace (±5°C) and either ice brine quenched (IBQ) or air quenched (AQ). After heat treatment, the sections were machined into standard Charpy V-notch impact specimens, Fig. 1a, or 1/4 in. diameter round by 1 in. gauge length tensile specimens, Fig. 1b. Spray coolant was used at all times to prevent overheating during the machining operations.

Aging studies were conducted on 1/8 in. sections of rod. These specimens were heated to 900°C for 2 hrs and IBQ from the as forged condition. This was followed by heating in a salt bath at the desired temperature (±2°C) for from 0.3 to 50 hrs and water quenching.

C. Mechanical Testing

1. Hardness Tests

A Wilson Rockwell Hardness Tester was used for all hardness measurements. The Rockwell "A" scale (60 kg major load and diamond Brale indentor) was used. A minimum of four hardness impressions were made on the notched face of each Charpy specimen, and the results averaged.

Scale and oxide was removed from the aged specimens by grinding on a 240 grit wet belt before testing. A minimum of four impressions

were made on the specimens and the results averaged.

2. Charpy Impact Tests

Charpy impact testing was conducted on a 225 ft-lb capacity Charpy impact testing machine with a hammer velocity of 16.9 ft/sec. Impact tests were conducted at 23°C, -78°C and -196°C. Crushed dry ice and liquid nitrogen (LN) were the coolants used at -78°C and -196°C, respectively. Specimens were impacted within 5 sec after removing from the cooling bath per ASTM E-23-64.[19] Two specimens were tested for each heat treatment and the angles corrected for pointer and air and bearing friction[20] before calculating energy absorbed in fracture. The impact values were then averaged.

3. Tensile Tests

Tensile properties were determined on an 11,000 lb capacity Instron Testing Machine at a crossheat speed of 0.02 in./minute. Tests were conducted at room temperature and -196°C (LN).

D. Dilatometry

Dilatometric studies were conducted to determine the $\alpha + \gamma$ region and the transformation characteristics of the material. The specimens were 1 in. long tubes with a 1/4 in. outside diameter and 1/32 in. wall thickness. These tubes were machined from the broken halves of Charpy impact specimens. Dilatometric curves were made by heating and cooling the specimens at 750°C/hr in an air atmosphere furnace and simultaneously recording the specimen expansion and its temperature.

E. X-Ray Diffraction

The retained austenite content was determined on transverse sections of both tested and untested Charpy bars using a Norelco type 12045 diffractometer with Cu-$K_{\alpha 2}$ (λ = 1.54050Å) radiation and monochromator. The surface to be scanned was polished and etched twice to remove any worked surface from the cutting operation. The scan was run from 2θ = 40° to 83°, and the intensity of the 110(44.7°) BCC and 111(42.8°), 200(49.8°) and 220(72.0°) FCC reflections determined and compared.

F. Microscopy

1. Optical Microscopy

Transverse sections of broken Charpy specimens were used for optical metallographic observation. These sections were mounted in Koldmount, abraded on silicon carbide papers to 600 grit, polished on a 1μ diamond wheel and final polished on an 0.05μ Al_2O_3 Vibromet. Specimens were etched in 75%-Kalling etch: 25% of 5% nital, mixed fresh. Etching time was 20 to 45 seconds.

2. Scanning Electron Microscopy

The fracture surfaces of selected Charpy specimens were examined with a Jeolco JSM-U3 scanning electron microscope (SEM) with secondary emission at 25 kV.

3. Transmission Electron Microscopy

a. Replicas

Replicas were taken from the surface of the etched optical specimens by the direct carbon technique. The carbon was evaporated at an angle of 30° off the surface normal. A solution of 10% HCl in ethyl

alcohol was used to separate the replica from the specimen surface. The replicas were examined with the Siemens 1A electron microscope operated at 60 kV.

b. Thin Foils

Thin foil samples suitable for transmission electron microscope examination were prepared by the standard window technique using an electrolyte of 75 gms of CrO_3 in 400 cc of acetic acid and 20 cc of H_2O. Specimens were examined in the Siemens 1A microscope operated at 100 kV.

III. EXPERIMENTAL RESULTS AND DISCUSSION

A. Toughness

The discussion will be divided into the following sections for presentation.

1. Structure and Properties of Optimally Heat Treated Specimens
2. Structure and Properties of Non-Optimally Heat Treated Specimens
   a. Heat treatments above the high toughness temperature range
   b. Heat treatments below the high toughness temperature range

1. Structure and Properties of Optimally Heat Treated Specimens

The toughness of this alloy is highest after heating for 2 hrs in the temperature range of 700°C to 750°C from the as forged (AF) or 900°C (2 hrs) AQ condition, Figs. 2 and 4 respectively. The microstructures corresponding to these conditions are shown in Figs. 5 and 7. On either side of this high toughness region (i.e., below 700°C or above 750°C) there is a sharp decrease in Charpy V-notch energy to below 20 ft-lb. Figures 8 and 9 show the fracture surfaces of the Charpy bars across the whole temperature range from 600°C to 900°C for these two conditions. They illustrate the large amount of plastic deformation occurring in the 700°C to 750°C temperature ranges and the flat, brittle fractures above and below this region. Scanning electron fractographs in Fig. 10 show the typical dimpled rupture of the high toughness heat treatments (Fig. 10c,d) and the cleavage and quasicleavage which dominates the low energy fractures (Fig. 10a,b,e,f). One inconsistent

result is the high toughness produced at 650°C from the as forged condition (Fig. 2). This topic will be discussed in Section 2b of the Discussion.

Dilatometric curves are shown in Fig. 11 for several cooling rates from 900°C and for the as forged condition. The conventional $\alpha \rightarrow \gamma$ start and finish temperatures (Ac_1 and Ac_3 temperature), as taken from these curves, are shown in Table 2. This data shows that the $\alpha \rightarrow \gamma$ transformation occurs between 666°C ± 3°C and 713°C ± 5°C on heating at rates of 180°C and 750°C/hr. Thus, the high toughness temperature range is seen to correlate well with the transformation $\alpha \rightarrow \gamma$ on heating. Further evidence of this is shown in Fig. 12 representing the kinetics of transformation and the resulting change in impact properties with isothermal treating at 650 to 800°C. The microstructures corresponding to these curves are shown in Figs. 13 to 18.

From Fig. 12 it is seen that the development of high toughness is a time and temperature dependent phenomenon. At 650°C, the structure is very stable (Figs. 13 and 14) with little improvement in toughness after 30 hrs at temperature. At 700°C the toughness requires over 1 hr to reach an optimum level. The microstructure at 700°C (Figs. 15 and 16) changes rapidly between 0.5 hrs and 6 hrs. Starting with a very fine dispersion of α and α' (retransformed γ)[21] at 700°C (0.5 hrs), the structure changes with time to islands of $\alpha + \alpha'$ surrounded by pure α' and then to almost 100% α' with small particles of α remaining untransformed. (Small amounts of α should be stable at equilibrium at

700°C, Fig. 19.[22]) The production of high toughness at 700°C closely parallels the amount of α' present, being low when the amount of α' is low and high when the structure is almost completely α' (nearly 100% γ at 700°C). This indicates that the toughness is dependent on the transformation or some product of the transformation (i.e., grain size change, substructure change, reduction in either segregation or the amount of brittle phases). At 750°C, less than 0.5 hrs is required to develop high toughness and the structure and properties are stable to 6 hrs at temperature.

There are several possible advantages to be gained from a low temperature phase change which could effect the low temperature properties of a material. Among these are a reduction in grain size, a change in substructure, a resolution of embrittling precipitates or grain boundary phases produced on cooling from the previous treatment, retention of small amounts of γ and a reduction in segregation or compositional variations between adjacent areas of the microstructure. Transmission thin foil work showed no evidence of precipitates in 900°C AQ material (Fig. 20) and no grain boundary networks. Microprobe analysis showed no composition changes in different grains or at grain boundaries so that any compositional variations have gradients of less than 1-2μ. X-ray diffraction studies of a variety of heat treatments indicated no measurable amount of retained γ.[21] This leaves only grain size and substructure effects to be responsible for the high toughness in the 700°C to 750°C range.

Figure 6 (the 900°C AQ + 650°C IBQ treatment) shows the 900°C grain diameter to average 75μ (ASTM GS 4.5). A subsequent 700°C (2 hrs) heat treatment produces a grain diameter of 9-11μ (ASTM 10.5) and at 750°C (2 hrs) a 10-12μ (ASTM 10) grain diameter. Grain size vs low temperature toughness results from Fig. 25 are summarized in Table 3. A grain diameter change of this magnitude would almost certainly reduce the NDT temperature.[14,15]

The substructure also undergoes a large change. At 900°C (Fig. 20) the substructure consists mostly of long parallel laths typical of massive martensite.[18,23,24] A subsequent heat treatment at 700°C or 750°C (Figs. 22 and 23 respectively) produces a structure more representative of equiax α in Fe-Ni alloys,[18] containing rounded subboundaries and areas of high and low dislocation densities as opposed to long, straight martensite laths. This lower temperature structure is very reminiscent of the "ideal" substructure mentioned in the Introduction, i.e., one consisting of a fine duplex substructure with alternate heavily dislocated and lightly dislocated areas.

Another important characteristic of this material is its characteristic of maintaining consistantly high impact properties with a wide range of cooling rates, as shown in Fig. 26. It is seen that the material is quite insensitive to cooling rate; the only effect being a slight increase in both hardness and toughness with decreasing cooling rate. Although no evidence has been found of precipitation on air quenching, the hardness increase at this cooling rate might be due to the clustering of nickel and titanium atoms.[28,33,34]

Although these initial stages of precipitation are seen to enhance both hardness and impact resistance, isothermal aging experiments have so far produced disappointing results. The hardening characteristics on isothermal aging at 410°C to 515°C for 0 to 50 hrs are shown in Fig. 27. There is a considerable hardness increase in this temperature range with the highest hardness for reasonable heating times occurring for treatments at 450°C for 10 to 25 hrs. However, aging specimens for 5 hrs at 450°C reduced the Charpy V-notch energy at -196°C from 140 ft-lb to 8 ft-lb. Hopefully, further experiments to thoroughly explore this strengthening mechanism will lead to methods capable of simultaneously producing increased strength and high toughness at low temperatures. (See Section 2b of the Discussion.)

2. Structure and Properties of Non-Optimally Heat Treated Specimens

a. Heat treatments above the high toughness temperature range.

A matter of interest in this material is the rapid decrease in low temperature toughness that occurs between 750°C and 800°C for all heat treatments. As shown in Figs. 5 to 7 and Tables 4 and 5, there is no obvious change in microstructure or tensile properties which could help explain this drastic reduction in impact properties. One must therefore look deeper for the answers.

Two factors which would certainly contribute to the decrease in toughness between 750°C and 800°C are the substantial increase in grain diameter at 800°C and a more subtle change in the dislocation substructure size and morphology. Figure 25 and Table 3 illustrate the grain sizes (GS) at 700°C to 800°C. These are shown to be 9-11μ at 700°C (ASTM GS 10.5), 10-12μ at 750°C (ASTM GS 10) and 21-25μ at 800°C

(ASTM GS 8.0). This constitutes a significant grain size change of 2 ASTM grain size numbers and would produce a shift of the NDT to higher temperatures at 800°C.[14,15]

Examining Fig. 10c-f shows that the gross fracture features, as revealed by the scanning electron microscope, correlate well with the grain size and optical microstructure. At 750°C the fracture surface is a completely dimpled rupture with an average dimple size of 10-15μ. This is quite close to the size of the average grain. At 800°C, the fracture exhibits combined dimpled rupture and quasi-cleavage, with the quasi-cleavage being the dominant fracture mode of the two. The fracture topography at 800°C seems to have features which are about 20-30μ in size. These fracture features are not distinct but do correlate rather well with the grain size of the matrix (Fig. 25).

The dislocation substructure also undergoes a small change in appearance. At 750°C, the substructure is quite similar to that of equiaxed α as described by Owen[18] with curved sub-boundaries and areas of low and high dislocation density. At 800°C, the substructure begins to take on a characteristic more indicative of massive martensite, i.e., straight parallel lath -like sub-boundaries with plates of high and low dislocation density material.

Several transformation modes are possible from $\gamma \rightarrow \alpha$ in Fe base alloys depending on the type and amount of elements added. In the Fe-Ni system three transformation modes are obtainable depending on the Ni content and cooling rate. At low nickel contents (less than 7 at.% Ni) the transformation is an equiaxed α type involving short range diffusion. If the cooling rates are extremely high (>15,000°C/sec), the thermally

activated equiaxed α transformation can be suppressed and an athermal shear type massive martensite transformation results.[23] Between 10 and 29 at.% Ni the transformation is of the massive martensite type for cooling rates above 5°C/min and with greater than 29% Ni the transformation is by the acicular martensite shear transformation.[18]

The Fe-12 Ni-0.5 Ti alloy does not seem to follow this pattern. At 700°C and 750°C, both the optical and transmission thin foil structures are more remeniscent of the equiaxed α structure than the massive martensite type. There are at least two possible reasons for this inconsistency; the effect of carbon and titanium on the equiaxed α and massive martensite transformations, and the effect of grain size on these reactions.

Several elements are known to slow the kinetics of the equiaxed α reaction and favor the massive martensite transformation; among these are nickel, chromium and carbon.[18,23,24,25] Carbon in small quantities can greatly effect the kinetics of the equiaxed α transformation. Higher carbon contents (0.001 to 0.005 wt% C[18,25]) effectively slow the equiaxed α transformation and favor the massive martensite transformation. In the Fe-12 Ni-0.5 Ti alloy, titanium, by its scavenging effect on the carbon, could reduce the effect of carbon on the kinetics of the equiaxed α reaction. This lower carbon content could allow the equiaxed α transformation to become dominant at cooling rates of 50°C/sec or so and explain the presence of the equiaxed α structure.

The effect of grain size on the equiaxed α and massive martensite transformations is not well understood. Owen and Wilson[26] present data showing that there is an abrupt change in transformation mode from the equiaxed α to the massive martensite type as the austenitizing temperature

is increased. This change in transformation mode is attributed to the grain size change with austenitizing temperature and its effect on the nucleation rate of the equiaxed α transformation. This γ grain size effect could also help explain the substructure change between 750°C and 800°C.

From the above considerations, it is thought that the loss in toughness between 750°C and 800°C is strongly related to the grain size increase occurring in this temperature range. The substructure as controlled by transformation mode changes are thought to play a less important role in determining the low temperature toughness of the alloy.

b. Heat treatments below the high toughness temperature range.

A second area of interest on the Charpy V-notch energy vs heat treat temperature curve is the low temperature decrease in properties which are seen to occur below 700°C after a 900°C treatment (Fig. 3,4) and below 650°C from the as forged condition (Fig. 2). This low temperature drop off is expected for two reasons. The starting material [900°C (2 hrs) AQ] has a Charpy V-notch energy of 9 ft-lb at -196°C and the value must rise smoothly from this value to that of the 700°C to 750°C value in some temperature interval, i.e., 650°C to 700°C. Also, as mentioned earlier, precipitation occurs rapidly on heating in the range of 450°C-500°C and above (Fig. 27), and this precipitation has been shown to be deterious to the low temperature toughness. What is unexpected is the abruptness of the transition and that the transition from brittle to ductile behavior at -196°C occurs at different heating temperatures for the AF and 900°C (2 hrs) AQ material.

The most likely answer to this problem can be found in the dilatometry data and optical microstructure. On studying the dilatometry curves it is seen that there is a point on each curve, well below the conventional Ac_1 temperature, where the expansion rate begins to differ from that of the ferrite. These points are given in Table 2. This phenomenon has been reported in other literature on Fe-Ni alloys[9] and is thought to be due to the precipitation of γ in the ferrite matrix below the conventional $\alpha+\gamma$ region on heating. This reverted γ is shown clearly in optical micrographs of the 650°C heat treatments as smooth, light areas in the matrix, Figs. 13b, 14b, 21b, 28 and 29.

The difference between the AF and 900°C AQ, plus a subsequent 650°C treatment, is seen to be in the way in which the γ precipitates in the α matrix. In the AF material (Fig. 28) the γ precipitates as spheroids, breaking up the α matrix and producing a very fine grained (5μ grain diameter) duplex structure of α and α' at room temperature. The structure is very homogeneous. When the 900°C AQ treatment is followed by a 650°C (2 hrs) IBQ or AQ treatment, the γ precipitates as needles or plates in the grain boundaries and along specific crystallographic directions in each grain (Fig. 21b). The previous 900°C grain size is not been broken up and there is an almost continuous film of α' along these grain boundaries. There is also no improvement in toughness over the original 900°C AQ structure. Both absorb 9 ft-lb at -196°C.

Figures 10a and b show scanning electron fractographs of the 900°C AQ and 900°C AQ + 650°C AQ charpy fractures. Here it is seen that the fracture features for both treatments are very similar in size and close to that of the 900°C AQ grain size (approximately 75μ). There

is less pure cleavage in the 650°C treated material and there is a very small amount of dimpled rupture present, most probably due to the α' needles, but the toughness is unchanged from that of the 900°C AQ material. The prior 900°C grain size seems to be controlling the fracture characteristics in both cases.

These differences in characteristics of precipitation of the γ, and the large grain size of the 900°C AQ material, are thought to be the reasons for the large difference in toughness between the AF and 900°C AQ materials when subsequently treated at 650°C.

The AF plus 650°C structure has a fine grained duplex structure of $\alpha+\alpha'$ without any continuous phase, while the 900°C + 650°C structure consists of large grains with a grain boundary envelope of α' and long needles of α' within the grains. This would seem to be a less favorable microstructure for resisting fracture at low temperatures.

On reviewing the hardness data (Figs. 2 through 4) and electron micrographs of the 650°C treated material the importance of being able to produce high toughness consistently at 650°C becomes obvious. Figures 2 to 4 show that there is a considerable increase in hardness at 650°C over the other heating temperatures so that if the high toughness at 650°C from the AF condition could be reproduced in the 900°C AQ material it would be advantageous. Figs. 21c and 30 are transmission thin foil micrographs of the AF + 650°C and 900°C + 650°C materials respectively. The significant feature here is that both contain precipitates in the untransformed α areas of the material. These rod shaped precipitates explain the increase in hardness at 650°C. More important, these precipitates do not seem to affect the low temperature

toughness in the AF + 650°C material, as the substructures are very similar in both materials. The AF + 650°C material is very tough, while the 900°C + 650°C material is brittle at -196°C. This fact lends credence to the idea that there should be ways to use precipitate particles in this system to increase strength without decreasing toughness.

B. Tensile Properties

1. As Quenched

Tensile properties at 23°C and -196°C are given in Tables 4 and 5 for the as forged + 650 to 850°C (2 hrs) IBQ and the 900°C (2 hrs) AQ + 650 to 850°C (2 hrs) AQ material. Typical stress-strain curves for the as forged + 650°C (2 hrs) IBQ and 900°C (2 hrs) AQ + 750°C (2 hrs) AQ materials are shown in Figs. 31 and 32.

In uniaxial tension tests this material is extremely ductile in all heat treatments tested at either 23°C or -196°C. The tensile data does not at all reflect the drastic changes in impact energy that occur in the 650°C to 700°C and 750°C to 800°C temperature ranges. Also, the yield and tensile strengths increase by nearly 50% in going from 23°C to -196°C without any significant loss in percent elongation or percent reduction in area.

There is very little uniform plastic deformation in this material, plastic instability and localized necking occur very soon after yield with all the elongation being produced in a small percentage of the original gauge length. This is indicative of a very low work hardening rate, further evidenced both by the small stress difference between the yield and ultimate strength and by the data on cold rolling presented in Fig. 33. Here it is seen that the material will withstand greater

than 80% cold reduction with only 20% increase in tensile strength. This material was cold rolled from 0.400 to 0.017 in. in thickness without annealing before cracking occurred.

Titanium seems to show a considerable solution strengthening effect. Speich and Swann[24] report an 0.2% yield stress of approximately 70,000 psi for Fe-12% Ni, whereas the values found in this study are over 90,000 psi for 0.2% yield stress.

2. Isothermal Aged at 450°C

Table 6 lists the tensile properties of this material at 23°C and -196°C after isothermally aging the material at 450°C for 0, 5 and 24 hrs from the 900°C (2 hrs) AQ + 750°C (2 hrs) IBQ condition.

There is a 25% increase in yield and tensile strength at 23°C and a 15% tensile strength increase and 25% yield strength increase at -196°C after aging for 24 hrs at 450°C. The elongation and reduction in area are similar to the 650°C treatment but with a higher yield strength and slightly higher tensile strength. Again, even though the material in the aged condition has very low notch toughness at -196°C, the elongation and reduction in area are extremely good. Notched tensile tests or higher strain rates would most probably produce better correlations with the Charpy data on low temperature ductility.

IV. SUMMARY AND CONCLUSIONS

1. The Fe-12 wt% Ni-0.5 wt% Ti BCC alloy exhibits excellent combinations of strength and toughness at -196°C. Yield strengths and Charpy V-notch energies of 140-150 ksi and 130-160 ft-lb at -196°C are attainable by a number of convenient heat treatments. This material does in fact develop strength and toughness combinations at -196°C superior to any of the presently available commercial alloys used for low temperature service.
2. High toughness at -196°C is developed by heating to 700°C-750°C for 2-6 hrs and IBQ or AQ after a 900°C (2 hrs) AQ treatment. From the as forged condition, high toughness is obtainable by a 650°C to 750°C heat treatment for 2 hrs or greater. This temperature region for production of high toughness at -196°C is closely related to the $\alpha \rightarrow \gamma$ phase transformation which occurs on heating between 666°C ± 3°C and 713°C ± 5°C.
3. The high toughness of this alloy is believed to be the result of bringing together into a single BCC alloy, the following characteristic
   a) a high nickel content
   b) an initially low interstitial content
   c) interstitial scavenging (by titanium)
   d) a fine grain size and a finely dispersed, dislocation substructure of high and low dislocation density areas (produced by a low temperature phase transformation)
4. Given the high nickel content and low interstitial content of this alloy, the toughness at -196°C is thought to be mostly dependent on the grain size of the material.

5. The high toughness produced on heating to 700°C or 750°C is a time dependent phenomenon closely paralleling the amount of γ formed at temperature. The development of maximum toughness requires heating for over 1 hr at 700°C and less than 0.5 hrs at 750°C.
6. The low temperature toughness decreases abruptly when the final heating temperature is below 700°C (650°C from the as forged condition) or above 750°C. The degradation in properties below 700°C is thought to be due to the presence of the previous 900°C grain structure, which is not been eliminated by the subsequent heat treatment below 700°C, and to the precipitation of a γ envelope at these prior 900°C grain boundaries and γ needles along specific crystallographic directions in the lattice.

   The decrease in toughness above 750°C is most probably due to the increase in grain diameter from 11μ at 750°C to 25μ at 800°C. A change in dislocation substructure from randomly shaped and oriented areas of high and low dislocation density to long straight massive martensite type laths is also observed to accompany the deterioration of properties.
7. Isothermal aging at 450°C increased the yield strength significantly but drastically reduced the low temperature toughness. However, the presence of precipitates in the high toughness AF + 650°C (2 hrs) IBQ material suggests that precipitation is not necessarily deleterious to the low temperature toughness.

V. RECOMMENDATIONS FOR FURTHER RESEARCH

There are several interesting aspects of this material which should be investigated to increase our knowledge of its behavior and to improve its already excellent properties. These include:

1. It would be invaluable to know the effect of carbon content and the amount of other interstitial and tramp elements on low temperature properties. Small amounts of S, P, Si, Mn, Al, C and N_2 are normally present in commercially prepared alloys and the effects of comparable levels of these elements on the properties of this alloy should be determined. Knowledge of the effect of C is especially necessary as this element, in small amounts, can effect the strength level on quenching, the $\gamma \rightarrow \alpha$ transformation mode, the $\alpha \rightarrow \gamma$ transformation temperature and the presence and/or amount of retained γ.
2. Step heating and quenching experiments should be performed to determine more exactly the reason for the high temperature decrease in toughness (above 750°C). By comparing the properties of the following four heat treatments from the 900°C (2 hrs) AQ condition it should be possible to determine whether this decrease is due to transformation type and/or temperature, grain size, and/or substructure changes or the final temperature before quenching.
    1. 800°C (2 hrs) AQ
    2. 750°C (2 hrs) AQ
    3. 750°C (1 hr) → 800°C (1 hr) AQ
    4. 800°C (1 hr) → 750°C (1 hr) AQ

3. The effect of lowering the nickel content to 10 wt% or less and the effect of partial substitution of manganese for nickel[27] on the low temperature impact properties should be determined. If either of these changes could be effected without destroying the low temperature toughness of the alloy they would significantly decrease the alloy cost and thereby increase its desirability as a commercial alloy. Care must be taken on substituting Mn for Ni for severe embrittlement can occur in Fe-Ni-Mn alloys.[28]

4. The NDT temperature of this material should be determined as a function of temperature and time at temperature. This data would shed light on whether the properties are a function of transformation on heating and cooling or are more dependent on grain size effects.

5. The effect of titanium on the transformation type and temperature of Fe-Ni alloys is not at present known. The temperature of transformation $\alpha \rightarrow \gamma$ and $\gamma \rightarrow \alpha$ influences the grain size, dislocation substructure and hardness of the alloy, and the transformation type can have profound effects on the mechanical properties. It would thus be advantages to know the role titanium plays in each of these areas.

6. Work should most definitely be performed to improve the response of the low temperature impact properties to isothermal aging. There are several methods by which this could be done.

   a. Since precipitates are not detrimental to the AF + 650°C (2 hrs) IBQ material, it would be advantageous to determine the effect of aging at 550°C to 650°C for short times (0.1 to 5 hrs) on the impact properties of the high toughness (700°C and 750°C) structures. Thus, it might be possible to raise their strength by high temperature aging without destroying the toughness of the material.

   b. Both titanium and aluminum form strengthening precipitates with Ni[29] and the two elements in combination are known to have a greater effect than that of either element separately. It would be useful therefore to determine the effects of additions of Ti (0 to 1 wt%) + Al (0 to 1 wt%) on the aged tensile and impact properties of the material, both at room temperature and -196°C.

   c. Molybdenum has the effect of changing the precipitation sites of Ni-Ti particles from grain boundaries to the matrix of maraging steels.[30] It would therefore be useful to determine whether this element in small quantities (less than 1 wt% Mo) can improve the low temperature impact properties of this alloy after isothermal aging in the 400°C to 550°C temperature range.

d. Fe-Ni-Ti alloys of high nickel content respond to aging in the γ.[31,32] The $\gamma \rightarrow \alpha$ transformation of this alloy, on cooling, occurs below 450°C so that it might be possible to improve strength and toughness by aus-aging at 450°C-550°C.

7. Thermal cycling through a phase transformation is a practical method for reducing grain diameter. This method could very likely be used to increase both strength and toughness of the alloy at -196°C and below. The effect of several cycles (1 to 5 times) at 600°C to 850°C for 0.25 to 2 hrs should therefore be investigated.

8. The properties of this material should be determined at temperatures below -196°C. Fe-Ni alloys tend to exhibit a more gradual transition from high to low toughness than other BCC alloys. The properties of this and related alloys might very possibly remain superior to existing cryogenic alloys to temperatures approaching 0°K.

ACKNOWLEDGEMENTS

The author wishes to express his thanks to Professor Victor F. Zackay and Professor Earl R. Parker for their encouragement and guidance during the course of this investigation. He also wishes to thank Dr. Mike Yokota, Ben Francis, Go Sasaki and David Atteridge for their assistance and many helpful discussions.

The assistance of the support staff of the Inorganic Materials Research Division was also greatly appreciated. In particular, the author wishes to thank J. A. Patenaude and Duane Newhart (machining), Phila Witherall, Doug Kreitz and Mamie Brown (photography), Gloria Pelatowski (line drawings) and Jean Wolslegel (manuscript preparation).

This research was performed under the auspices of the U. S. Atomic Energy Commission through the Inorganic Materials Research Division of the Lawrence Berkeley Laboratory.

REFERENCES

1. F. R. Schwartzberg, Metal Progress 96, 52 (July 1969).
2. D. V. Lebedev and B. M. Ovsyannikov, Metal Science and Heat Treatment, 818 (1967).
3. A. P. Gulyaev and A. M. Fatkina, Metal Science and Heat Treatment, 817 (1966).
4. Metal Progress Data Book, 71 (1969).
5. C. W. Marshall, et al., Transactions of the ASM 55, 135 (1962).
6. Low Temperature Data Sheet, Types 304 and 304 L Stainless Steel, International Nickel Co. (1963).
7. E. A. Ul'yanin, Metal Science and Heat Treatment, 837 (1966).
8. F. R. Schwartzberg, Cryogenic Materials Data Book (Martin Co., Aug. 1964).
9. G. R. Brophy and A. J. Miller, Transactions of the ASM 41, 1185 (1949).
10. T. Oôka, et al., Kinzoku Gakkai-Shi 30, 435 (1966).
11. E. A. Ul'yanin and A. M. Fatkina, Metal Science and Heat Treatment, 439 (1967).
12. W. Jolley, J. of the Iron and Steel Institute 201, 170 (1963).
13. W. C. Benzer, American Machinist Special Report #618, 108 (1968).
14. R. L. Smith, et al., Transactions of the ASM 46, 973 (1954).
15. J. M. Hodge, et al., AIME Metals Transactions 185, 233 (1949).
16. N. F. Stoloff, Fracture of Metals, Ed. H. Liebowitz, Vol. 6, p. 1, 1969.
17. W. C. Leslie, et al. AIME Metals Transactions 218, 699 (1960).
18. W. S. Owen, et al., High Strength Materials, Ed. V. F. Zackay, 167, 1965.
19. ASTM E-23-64, ASTM Standards, part 30, p. 229 (1965).

20. H. E. Davis, et al., The Testing and Inspection of Materials (McGraw-Hill, Inc., 1955).

21. N. P. Allen and C. C. Earley, J. of Iron and Steel Institute 166, 281 (1950).

22. G. R. Speich, AIME Metals Transactions 227, 754 (1963).

23. W. D. Swanson and J. G. Parr, J. of the Iron and Steel Institute 202, 104 (1964).

24. G. R. Speich and P. R. Swann, J. of Iron and Steel Institute 203, 480 (1965).

25. M. J. Bibby and J. G. Parr, J. of the Iron and Steel Institute 202, 100 (1964).

26. W. S. Owen and E. A. Wilson, Iron and Steel Institute Report No. 93, 53 (1965).

27. W. R. Patterson and L. S. Richardson, Transactions of the ASM 59, 71 (1966).

28. M. D. Perkas and V. I. Snitsar, Physics of Metals and Metallography 17 [ ], 400 (1964).

29. S. Floreen, Transations of the ASM 57, 38 (1964).

30. S. Floreen and G. Speich, Transactions of the ASM 57, 714 (1964).

31. K. A. Malyshev and M. M. Vasilevskaya, Physics of Metals and Metallography 18, 150 (1964).

32. G. P. Kulinichev and M. D. Perkas, Physics of Metals and Metallography 29 [5], 128 (1970).

33. A. F. Yedneral, et al, Physics of Metals and Metallography 24 [4], 85 (1967).

34. V. M. Kardonskiy and M. D. Perkas, Physics of Metals and Metallography 19 [2], 133 (1965).

Table 1. Chemical composition of ingots used in this study (wt%).

Ingot #	Ni	Ti	Mn	C	S	P	N_2	Fe
708-16	12.10	0.51	0.005*	0.006	0.004	0.005*	0.003	Balance
722-10	12.35	0.54	0.005*	0.006	0.004	0.005*	0.004	Balance
726-13	12.05	0.47	0.005*	0.012	0.004	0.005*	0.004	Balance

*Indicates less than

Table 2. Dilatometry data for Fe-12 Ni-0.5 Ti (heating and cooling rate 750°C/hr).

Heat Treatment	Begin Transformation	Conventional Ac_1	Ac_3	Ar'	Ar"
As Forged	535°C	667°C	718°C	435°C	371°C
AF+900°C(2hrs)IBQ	542°C	663°C	716°C	442°C	382°C
AF+900°C(2hrs)AQ	560°C	669°C	709°C	459°C	390°C
AF+900°C(2hrs)+ Furnace Cool at 0.5°C/min	564°C	665°C	711°C	457°C	387°C

Table 3. Effect of heat treatment at 650°C to 800°C on grain size and charpy V-notch energy.

	Heat Treatment				
	900°C (2 hrs) AQ	900°C (2 hrs) AQ + 450°C (2 hrs) AQ	900°C (2 hrs) AQ + 700°C (2 hrs) AQ	900°C (2 hrs) AQ + 750°C (2 hrs) AQ	900°C (2 hrs) AQ + 800°C (2 hrs) AQ
Toughness (ft-lb at -196°C)	9	9	140	150	25
Grain Diameter	75μ	75μ	10μ	11μ	23μ
ASTM Grain Size	4.5	4.5	10.5	10	8

Table 4
Variation of tensile properties of Fe-12 wt% Ni-0.5 wt% Ti alloy with temperature for 3 heat treatments.

		Heat Treatment		
		650°C (2 hrs) IBQ	750°C (2 hrs) IBQ	850°C (2 hrs) IBQ
23°C	Tensile Strength (psi)	108,500	98,600	98,300
	0.2% Yield Strength (psi)	95,400	90,300	90,800
	% Elongation	22	21	21
	% Red. Area	81	84	86
-196°C	Tensile Strength (psi)	170,800	153,000	150,500
	0.2% Yield Strength (psi)	150,000	139,500	140,000
	% Elongation	20	18	21
	% Red. Area	74	75	74

*1 inch gauge length by 0.250 inch diameter specimen.

Table 5
Variation of tensile properties of Fe-12 wt% Ni-0.5 wt% Ti alloy with temperature for 3 heat treatments.

		Heat Treatment		
		900°C (2 hrs) AQ +650°C (2 hrs) AQ	900°C (2 hrs) AQ +750°C (2 hrs) AQ	900°C (2 hrs) AQ +850°C (2 hrs) AQ
23°C	Tensile Strength (psi)	114,500 psi	100,000 psi	100,000 psi
	0.2% Yield Strength (psi)	107,500 psi	92,500 psi	93,400 psi
	% Elongation *	20%	23%	21%
	% Red. Area	84%	86%	87%
-196°C	Tensile Strength (psi)	168,000 psi	151,400 psi	152,000 psi
	0.2% Yield Strength (psi)	154,500 psi	139,300 psi	138,000 psi
	% Elongation *	20%	26%	24%
	% Red. Area	71%	78%	75%

*1 inch gauge length by 0.250 inch diameter specimen.

Table 6. Variation of tensile properties of Fe-12 wt% Ni-0.5 wt% Ti alloy aging at 450°C after a 900°C (2 hrs) AQ + 750°C (2 hrs) IBQ heat treatment.

		Time at 450°C (hrs)		
		0	5	24
23°C	Tensile Strength	100,000	113,000	126,000
	Yield Strength	92,500	106,000	120,000
	% Elongation*	23%	27%	25%
	% Red. Area	86%	83%	81%
-196°C	Tensile Strength	151,400	162,000	176,000
	Yield Strength	130,300	157,000	171,000
	% Elongation*	26%	23%	21%
	% Red. Area	78%	77%	72%

*1 inch gauge length by 0.250 in. diameter specimen.

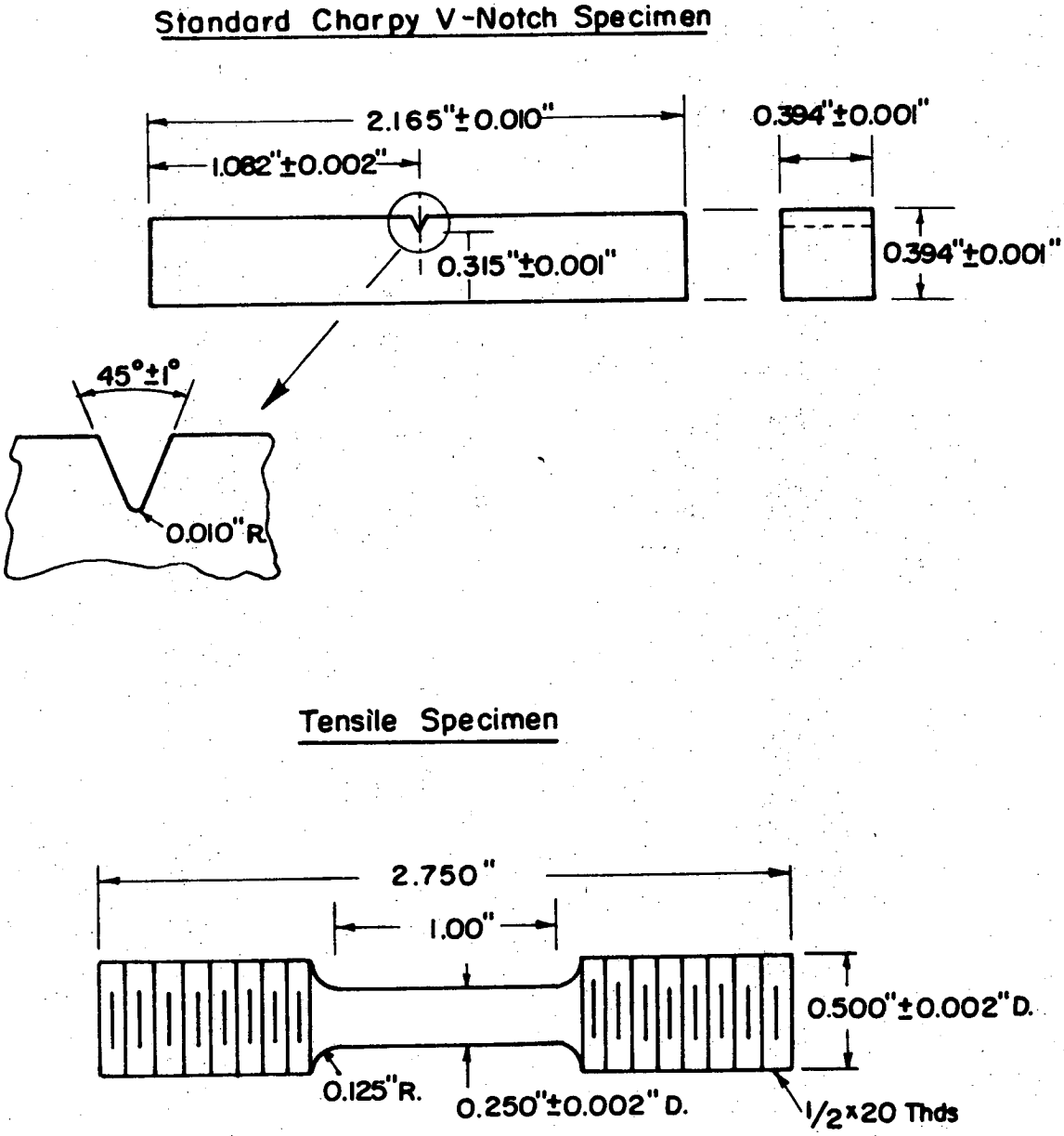

Fig. 1 Mechanical test specimens.

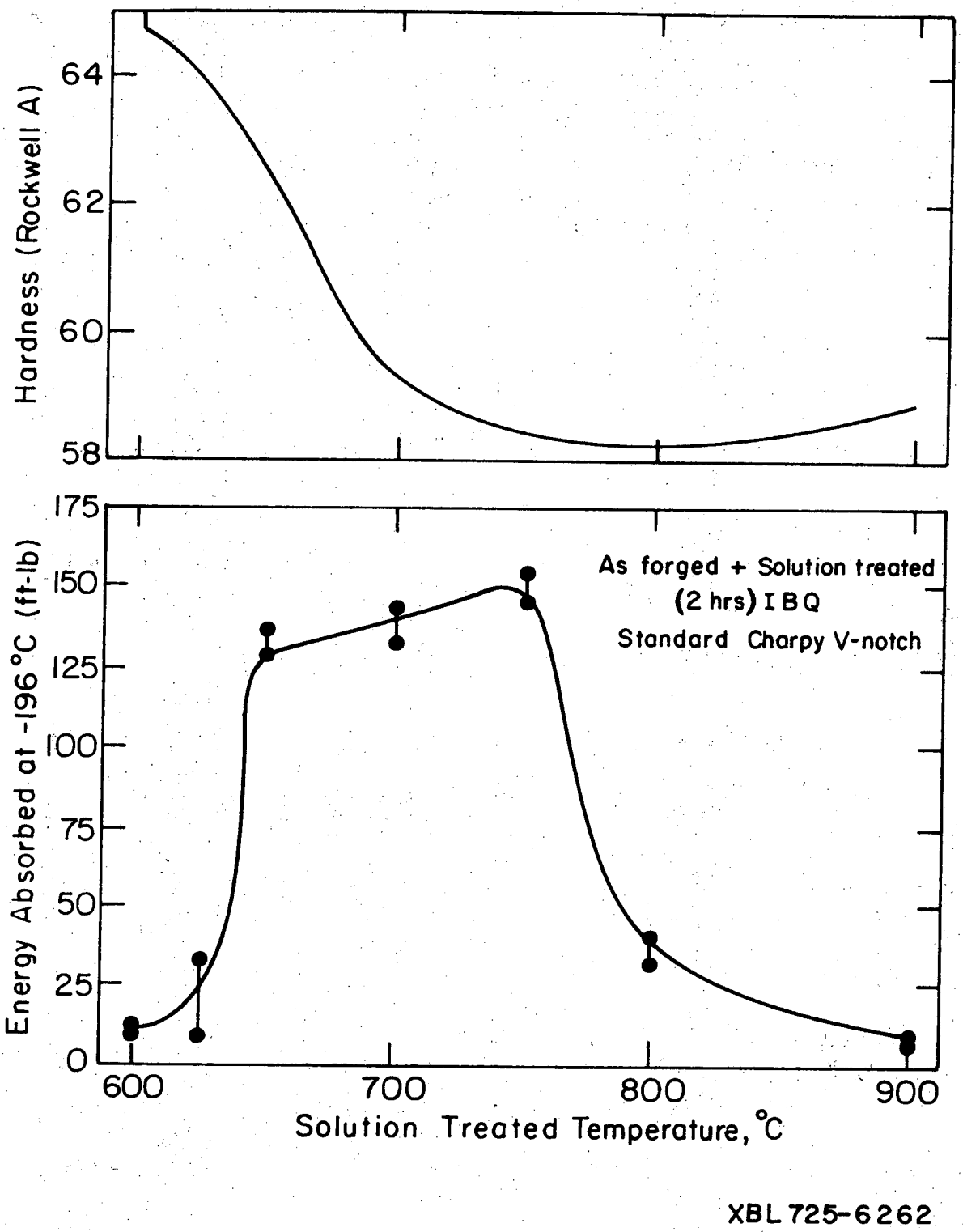

Fig. 2. Charpy impact energy at -196°C and hardness vs temperature from the as forged condition.

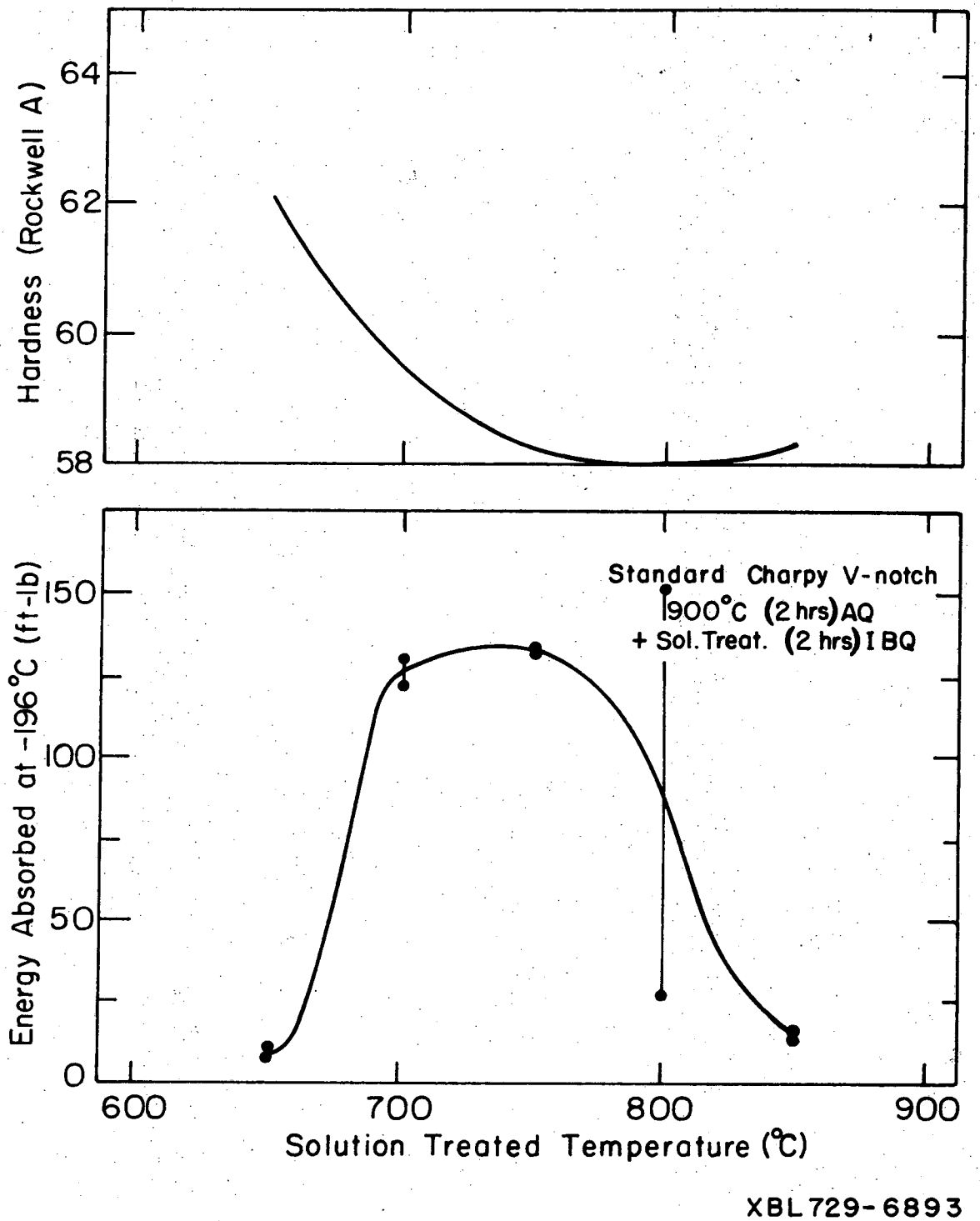

Fig. 3. Charpy impact energy at -196°C and hardness vs temperature + IBQ for the 900°C(2 hrs)AQ condition.

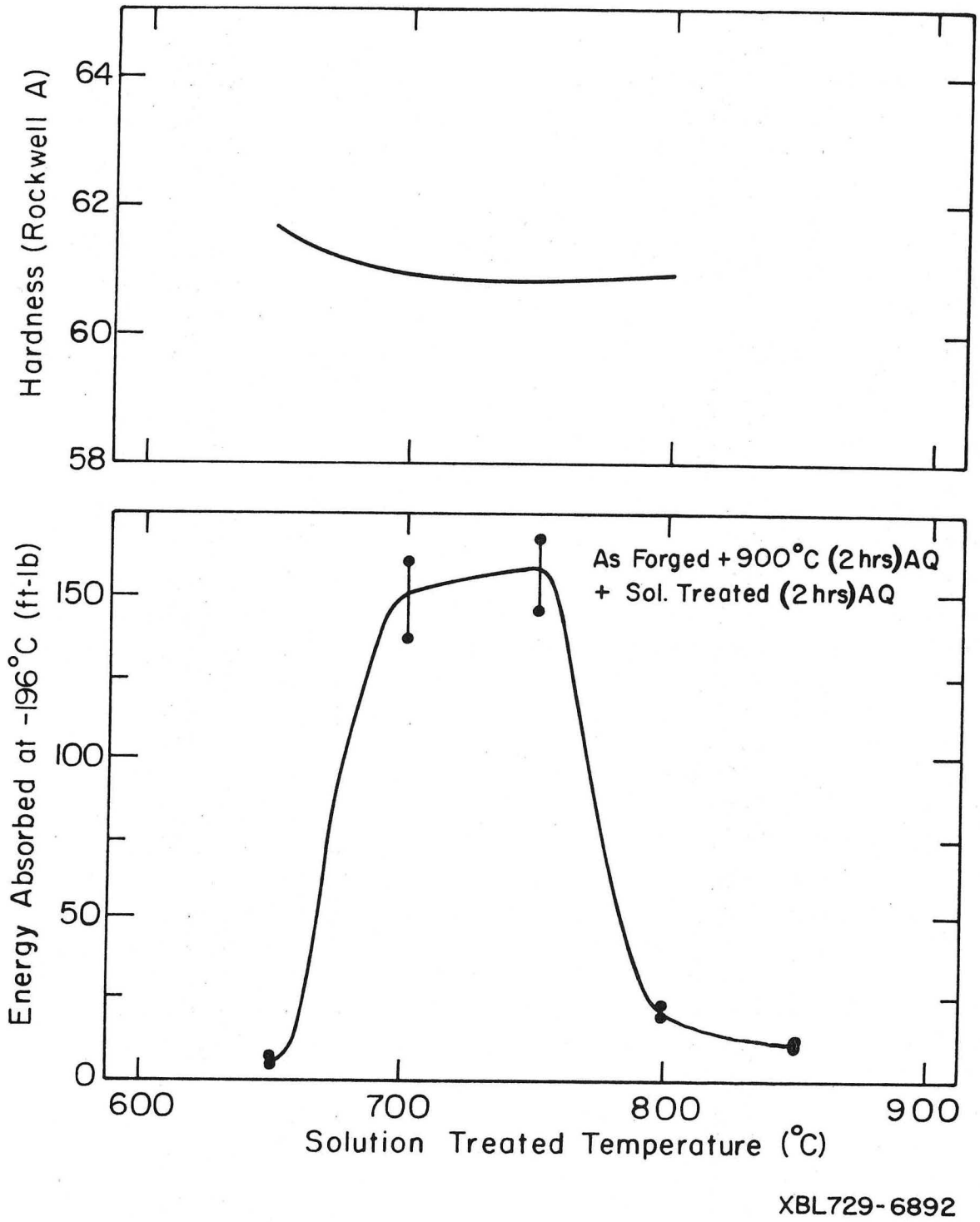

Fig. 4. Charpy impact energy at -196°C and hardness vs temperature + AQ for the 900°C (2 hrs) AQ condition.

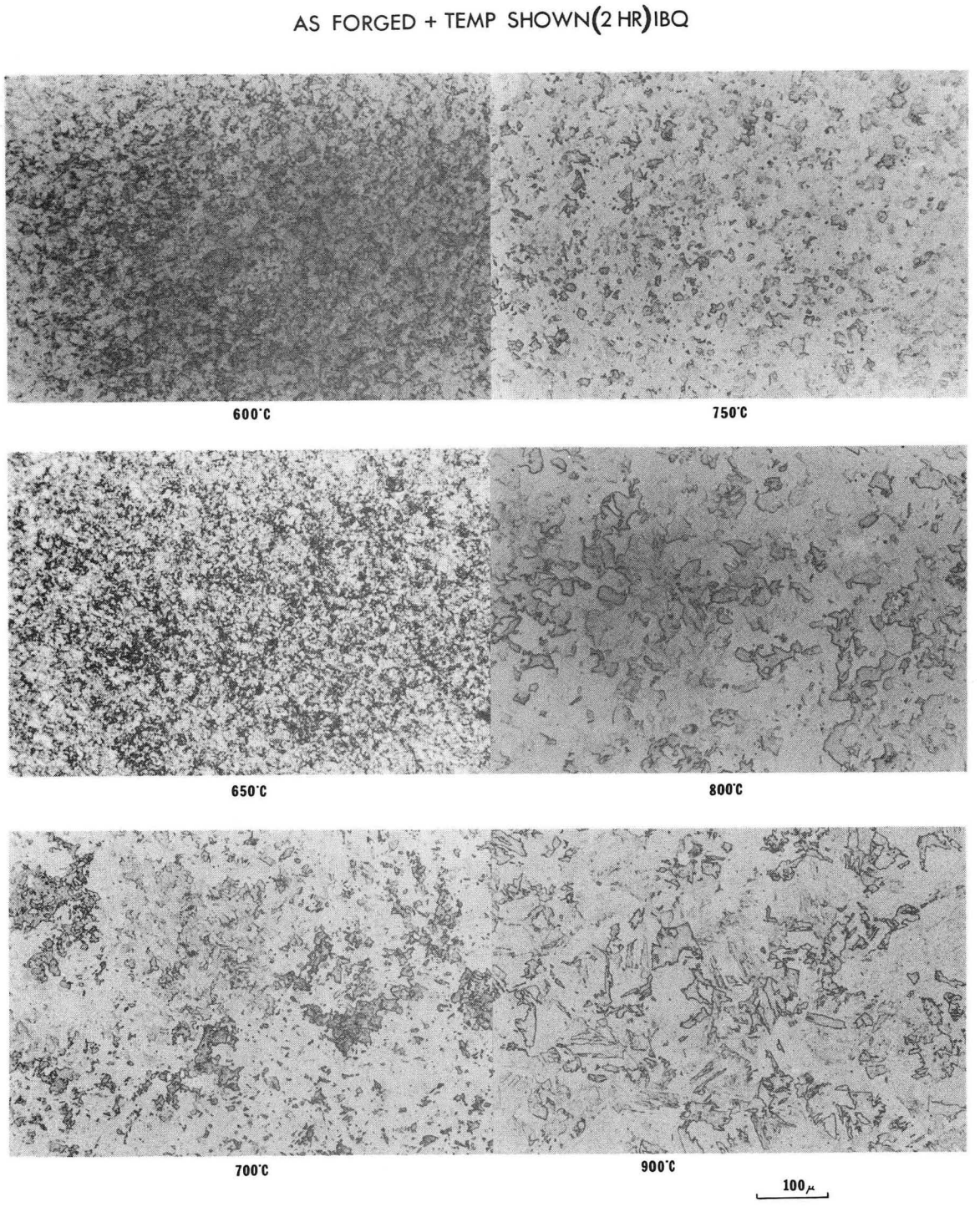

Fig. 5. Optical micrographs of as forged + 600°C to 900°C (2 hrs) IBQ heat treatments.

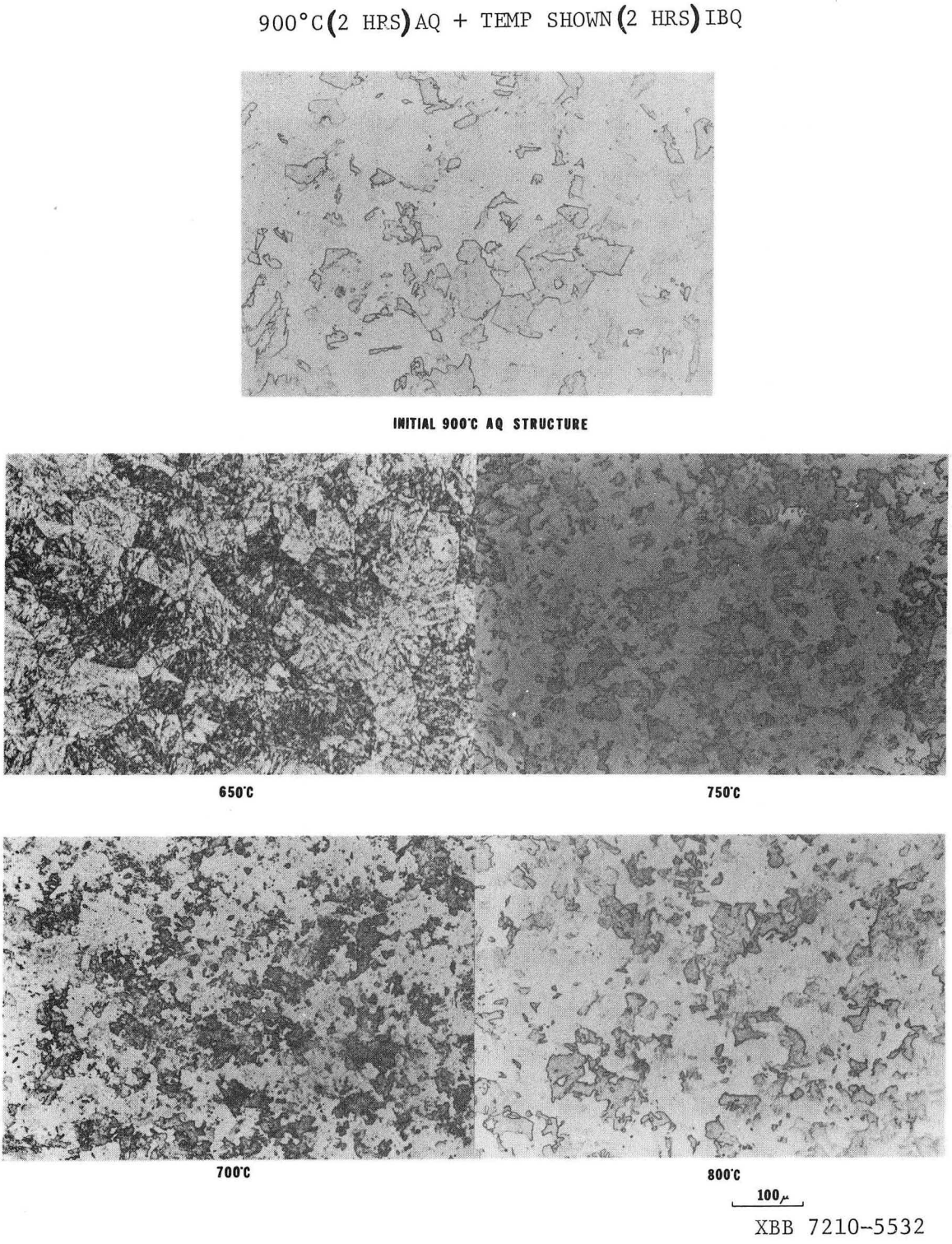

Fig. 6. Optical micrographs of 900°C (2 hrs) AQ + 650°C to 800°C (2 hrs) IBQ heat treatment.

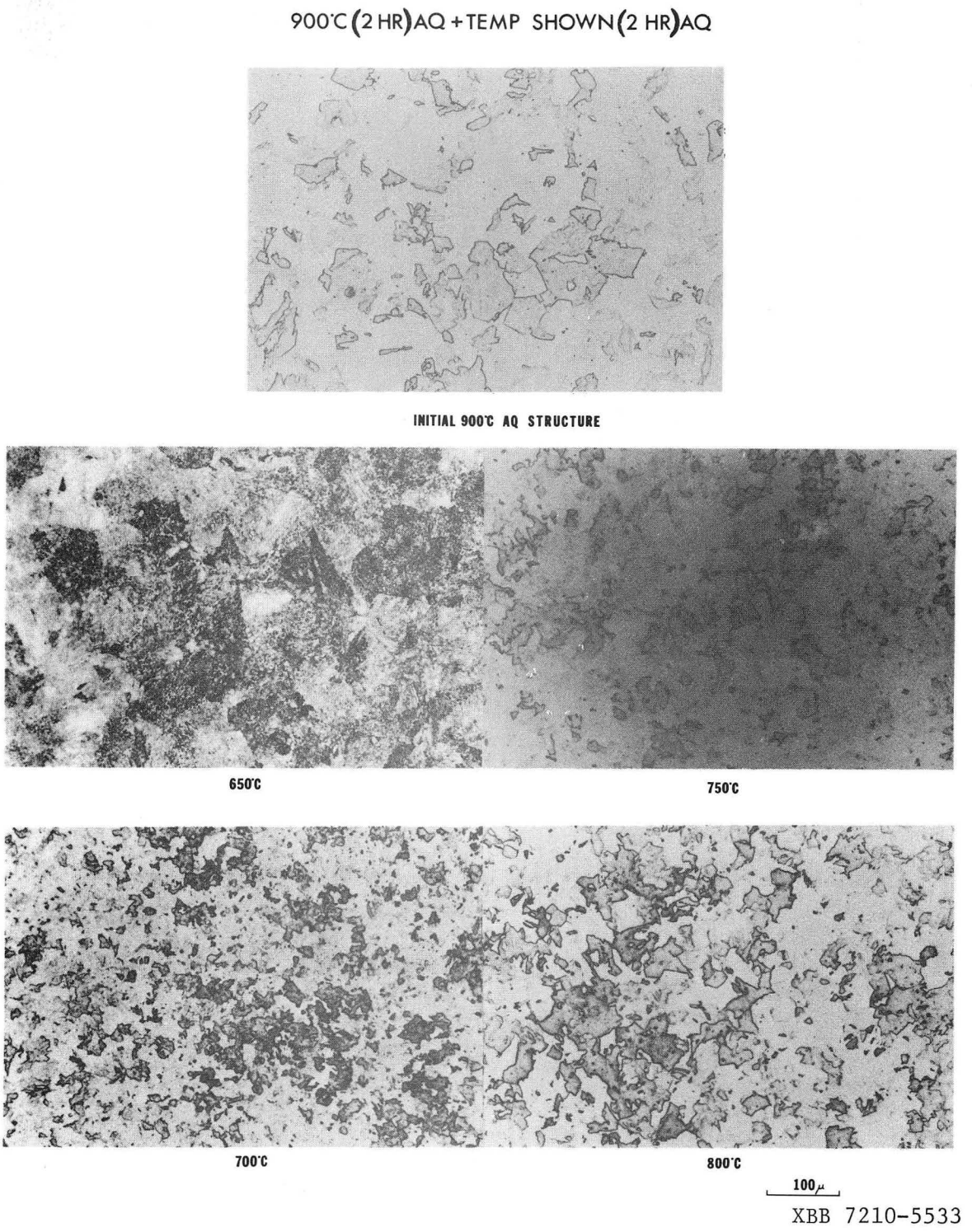

Fig. 7. Optical micrographs of 900°C (2 hrs) AQ + 650°C to 800°C (2 hrs) AQ heat treatments.

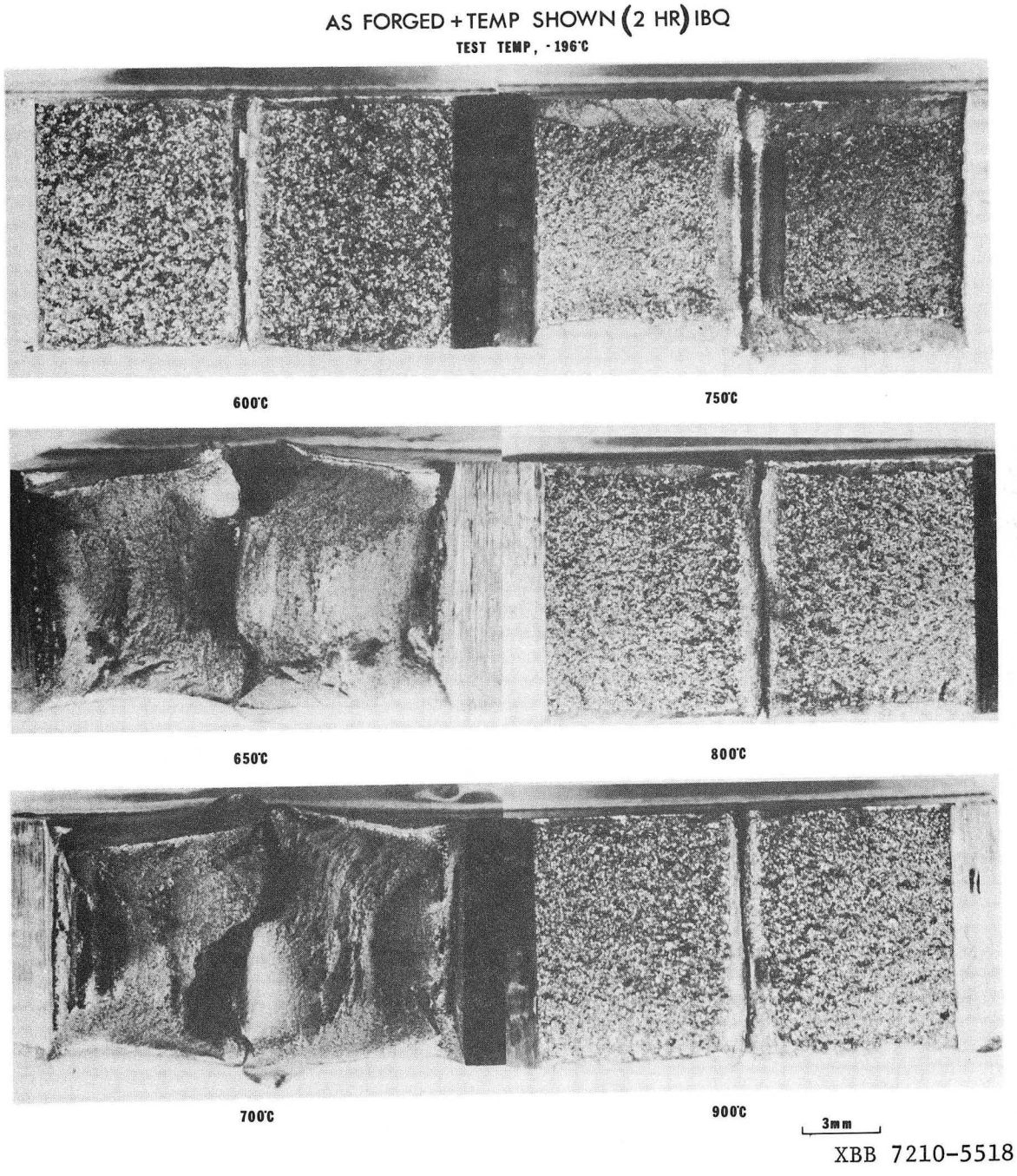

XBB 7210-5518

Fig. 8. Fractographs of as forged + 650°C to 900°C (2 hrs) IBQ Charpy fracture surfaces.

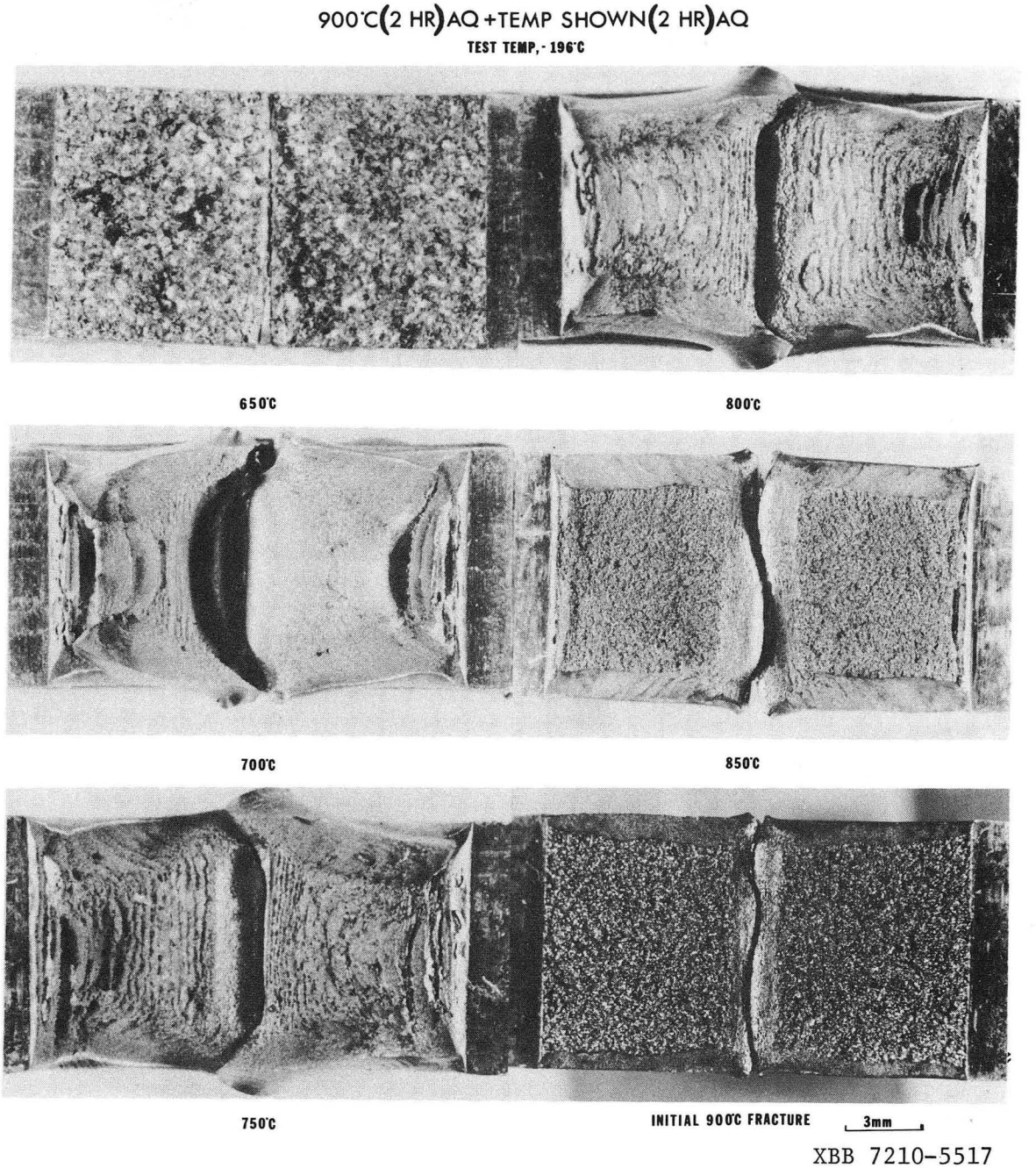

XBB 7210-5517

Fig. 9. Fractographs of 900°C (2 hrs) AQ + 650°C to 850°C (2 hrs) AQ Charpy fracture surfaces.

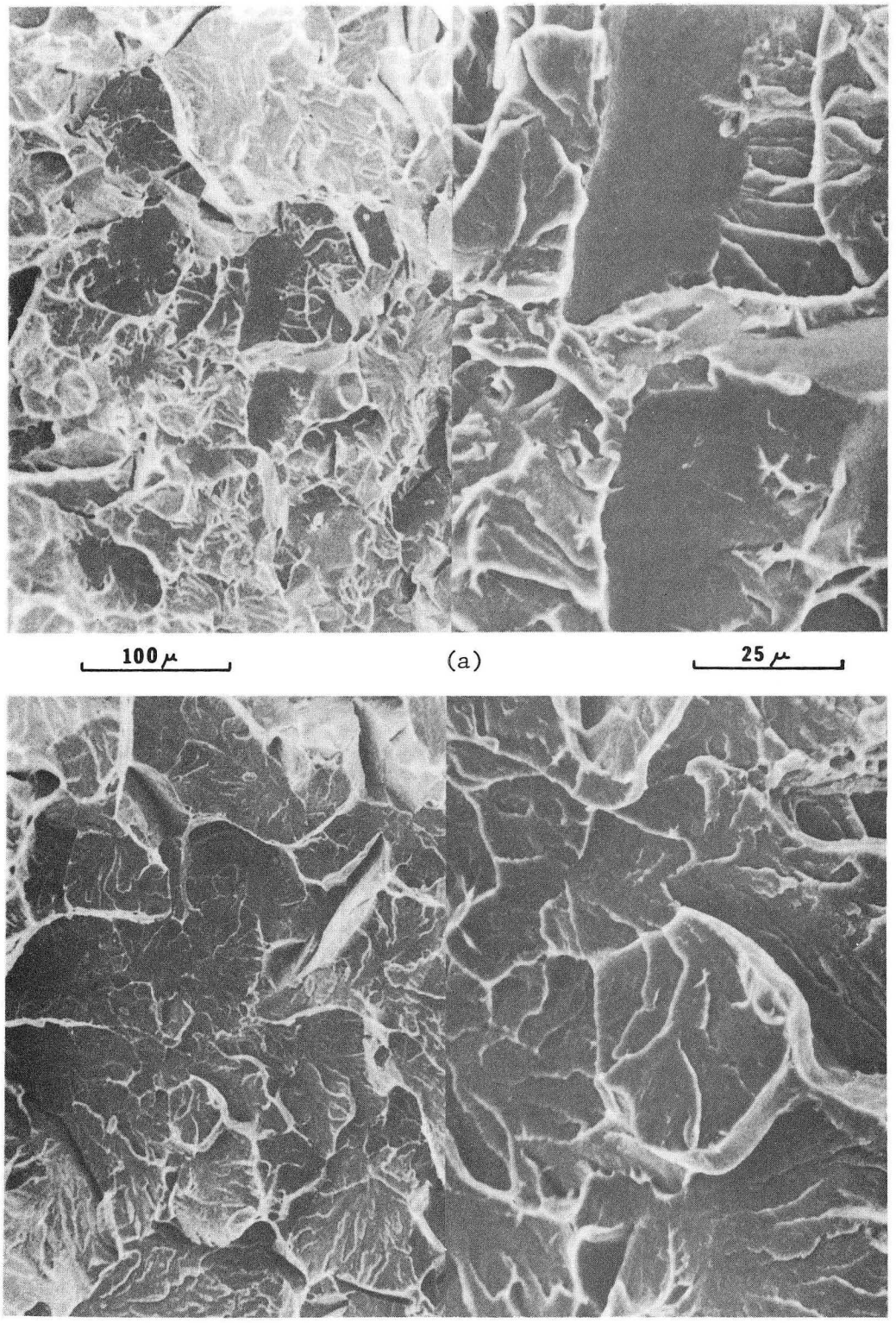

Fig. 10. Scanning electron fractographs of (a) 900°C (2 hrs) AQ and (b) 900°C (2 hrs) AQ + 650°C (2 hrs) AQ Charpy fracture surfaces.

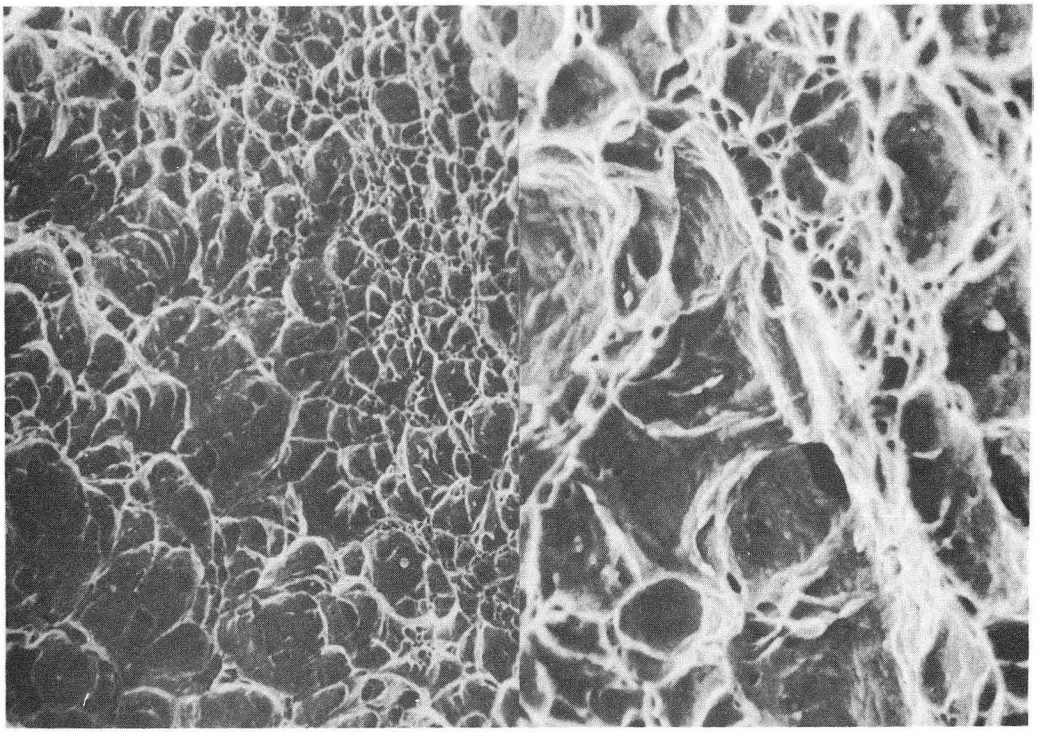

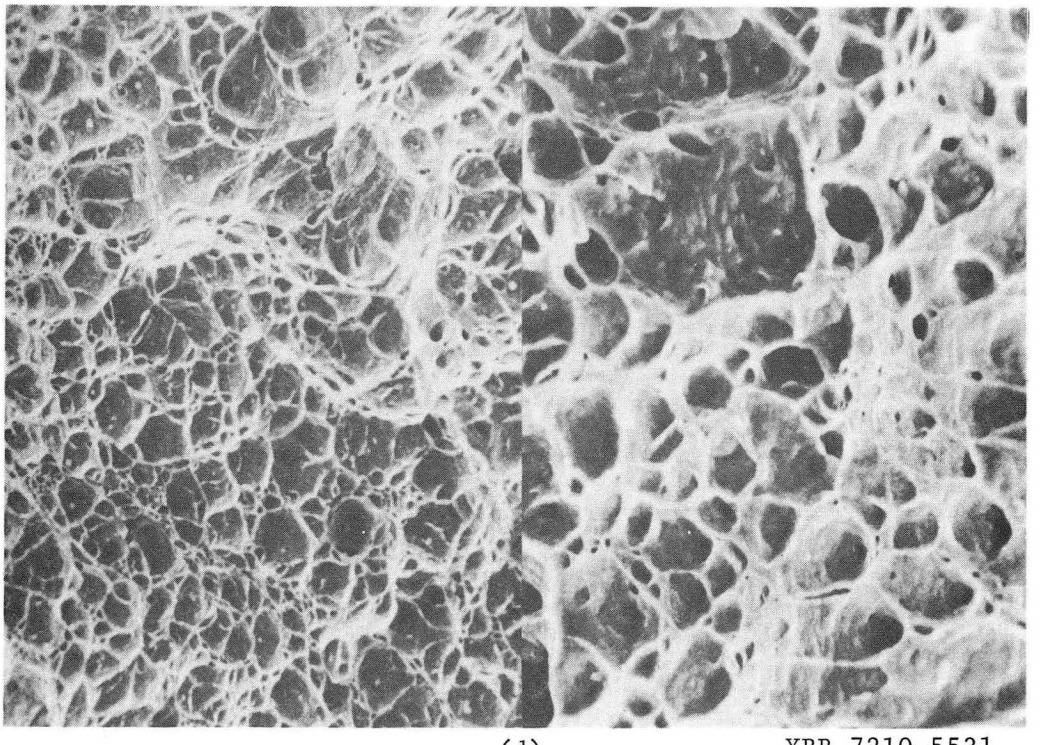

Fig. 10 continued
Scanning electron fractographs of 900°C (2 hrs) AQ + (c) 700°C (2 hrs) AQ and (d) 750°C (2 hrs) AQ Charpy fracture surfaces.

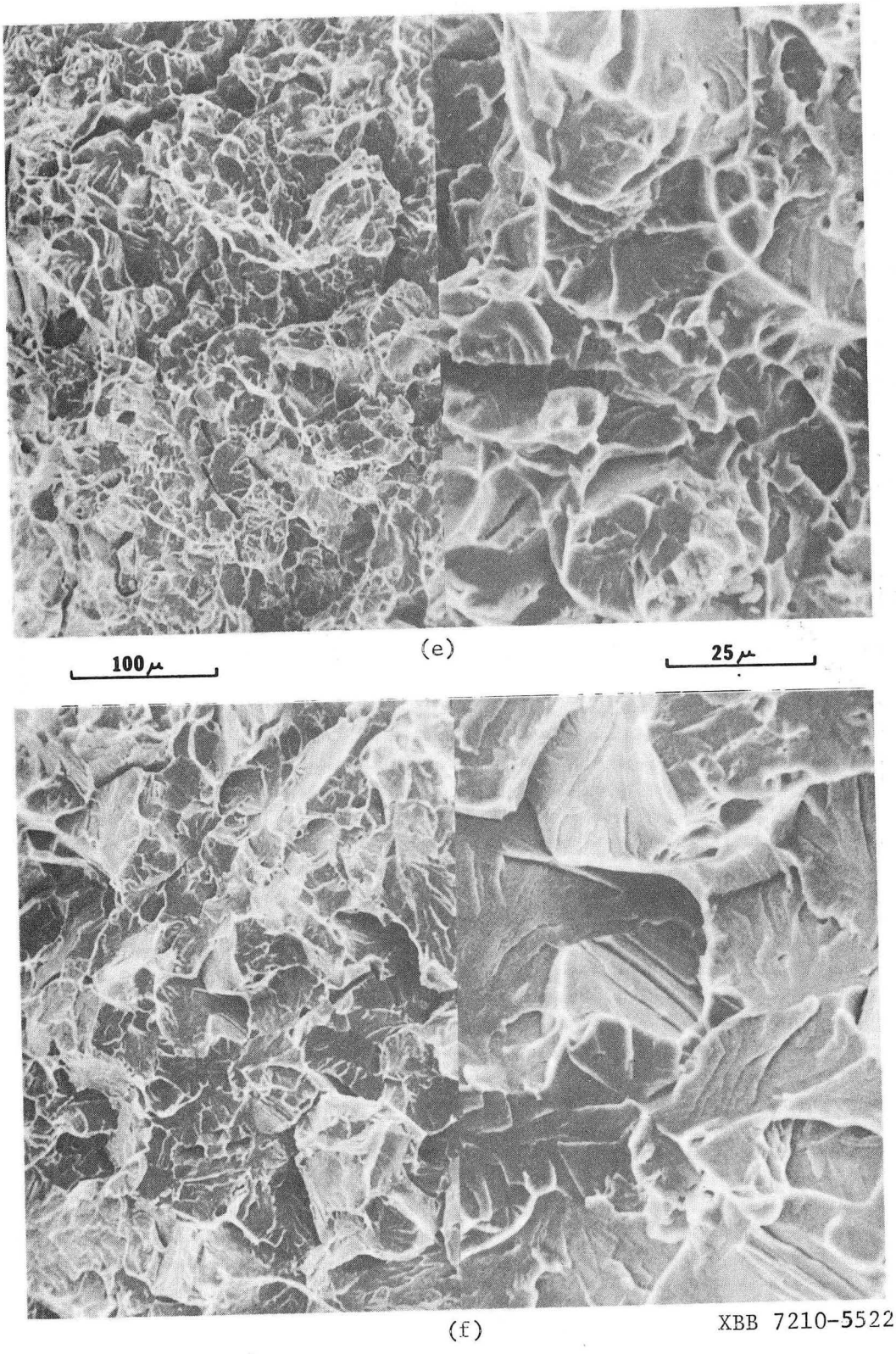

Fig. 10 continued
Scanning electron fractographs of 900°C (2 hrs) AQ + (e) 800°C (2 hrs) AQ and (f) 850°C (2 hrs) AQ Charpy fracture surfaces.

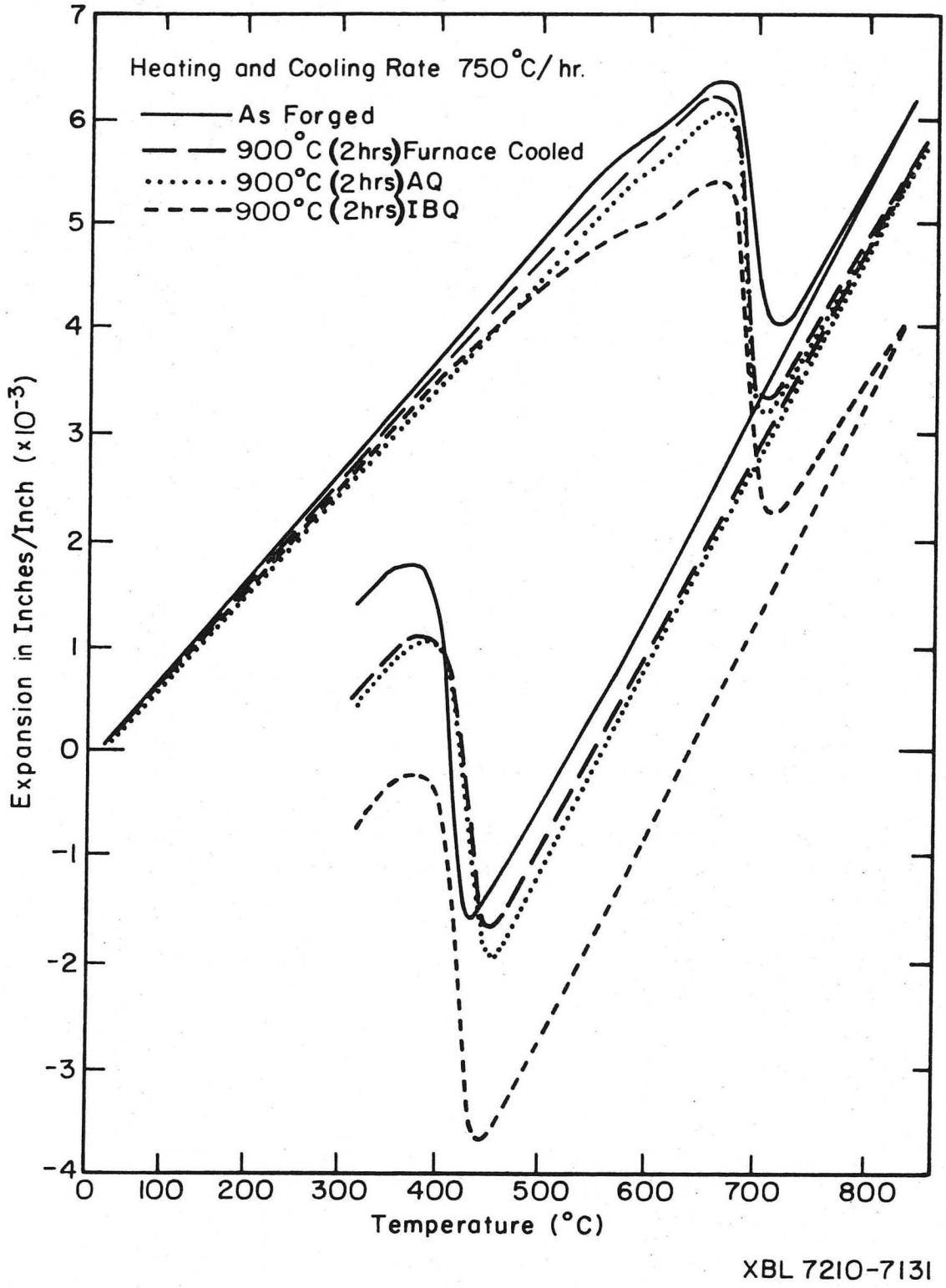

Fig. 11. Dilatometric heating and cooling curves for four heat treatments.

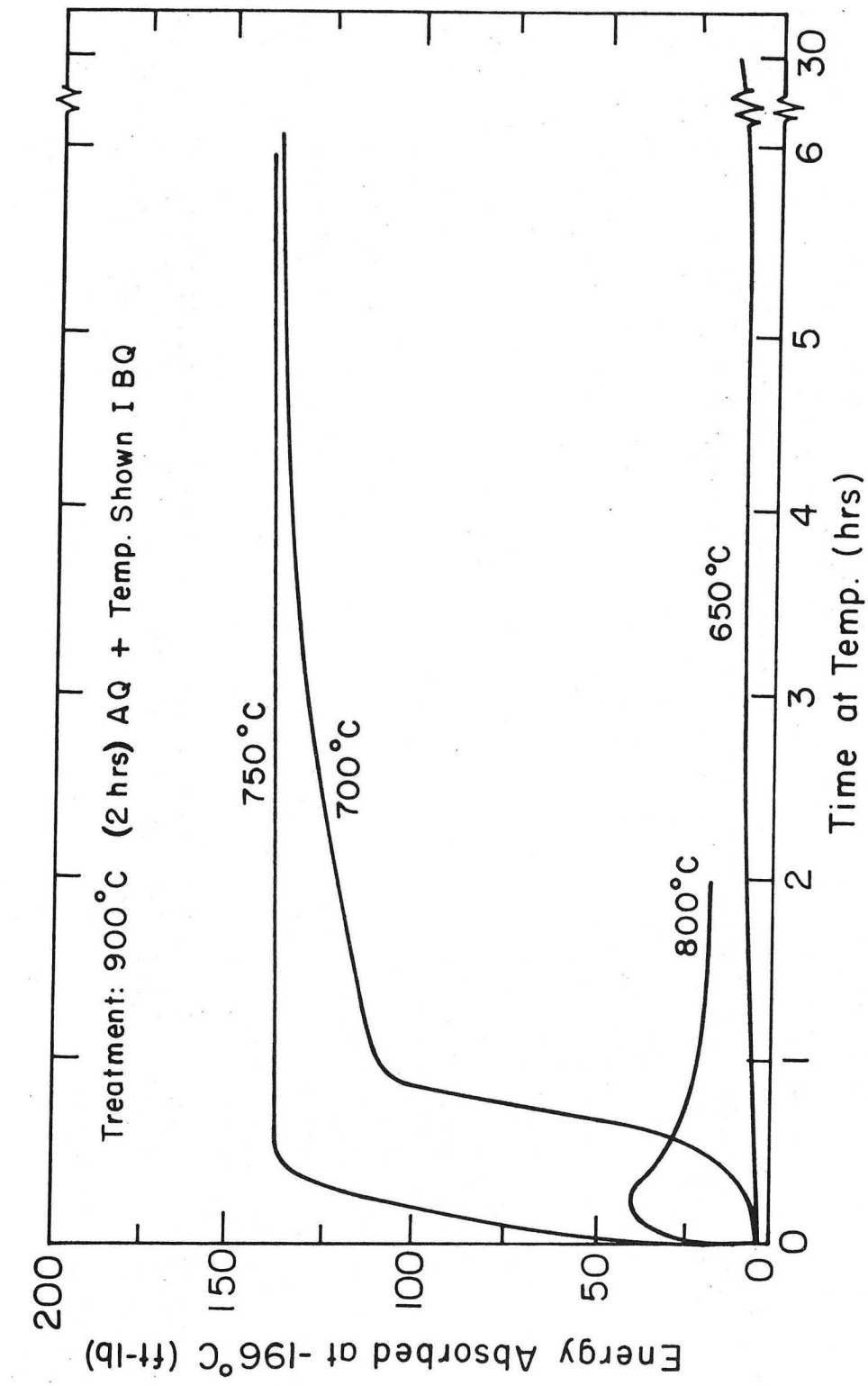

Fig. 12. Charpy impact energy of -196°C vs time at temperatures for four temperatures from the 900°C(2 hrs)AQ condition.

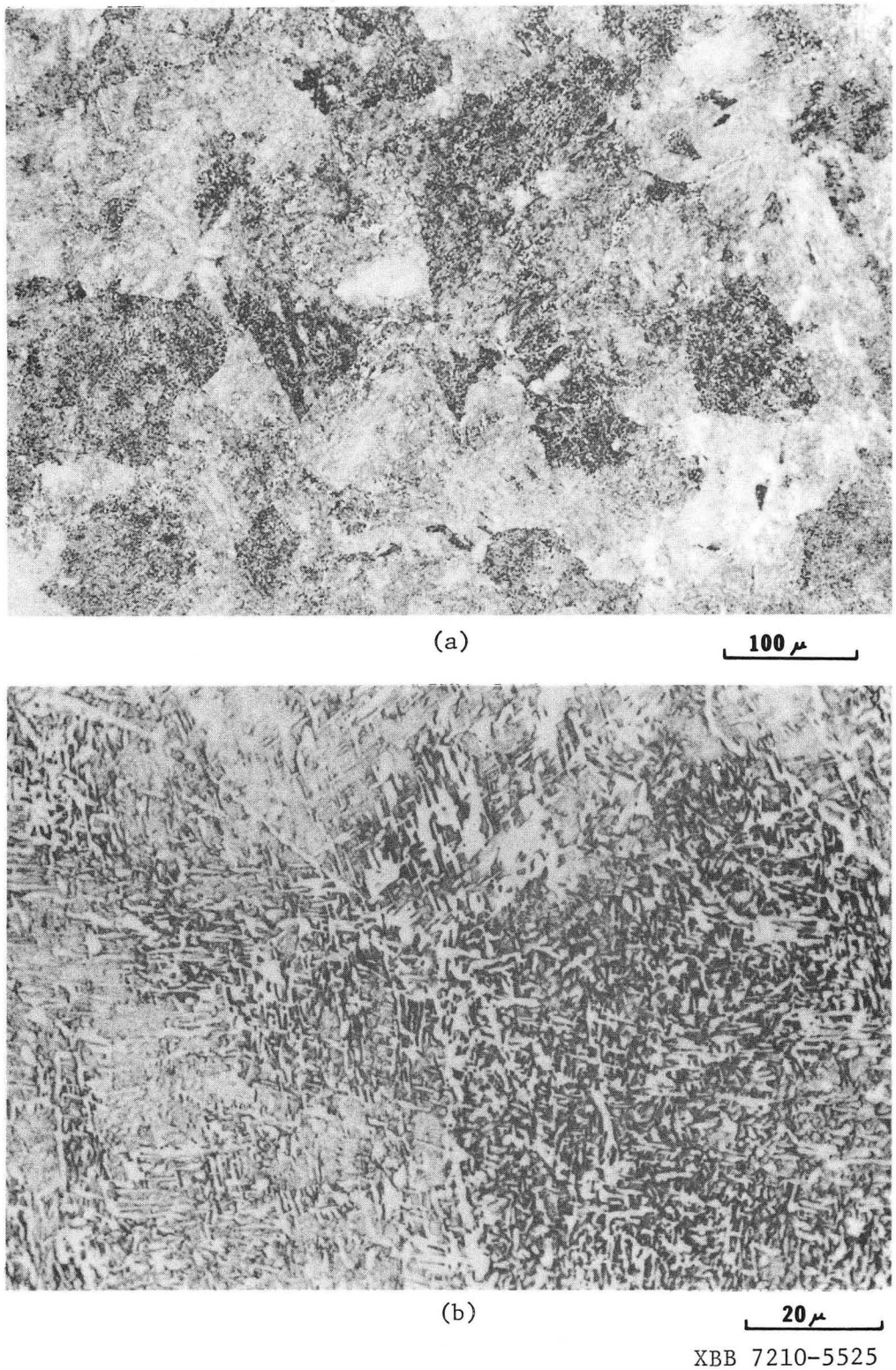

Fig. 13. Optical micrographs of 900°C (2 hrs) AQ + 650°C (2 hrs) IBQ heat treatment.

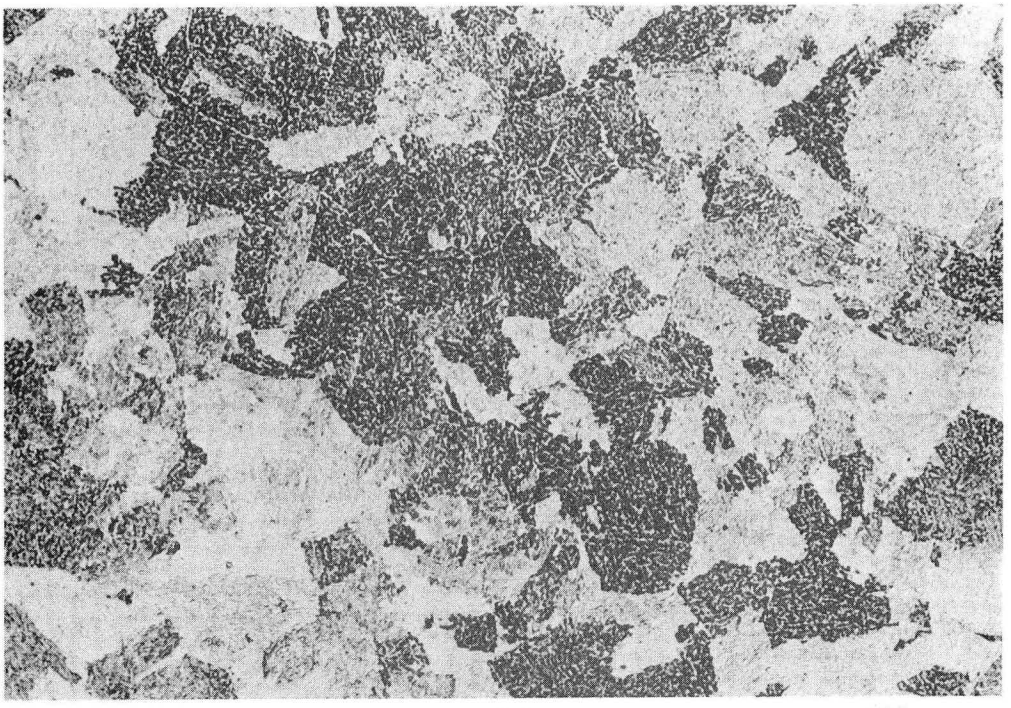

(a) 100 μm

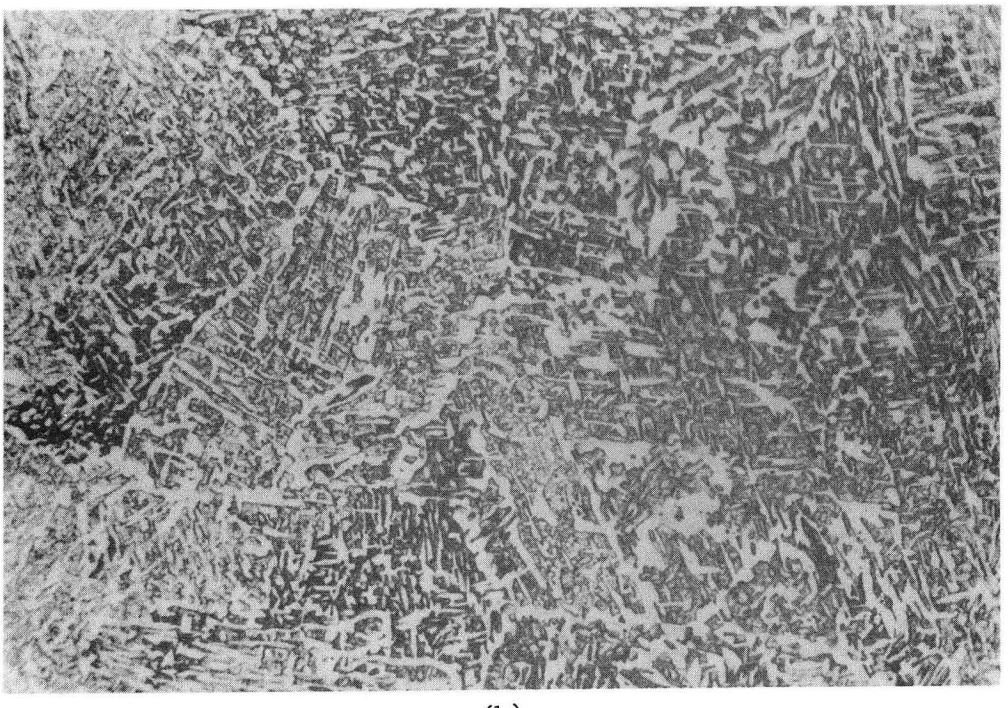

(b) 20 μm

XBB 7210-5528

Fig. 14. Optical micrographs of 900°C (2 hrs) AQ + 650°C (30 hrs) IBQ heat treatment.

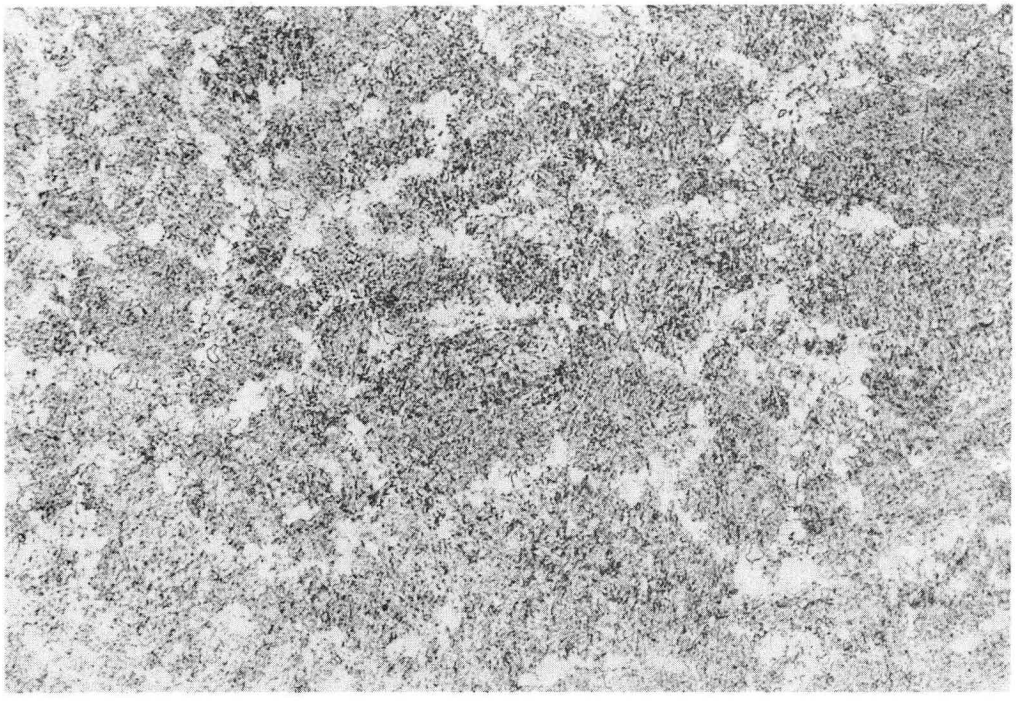

(a)

100μm

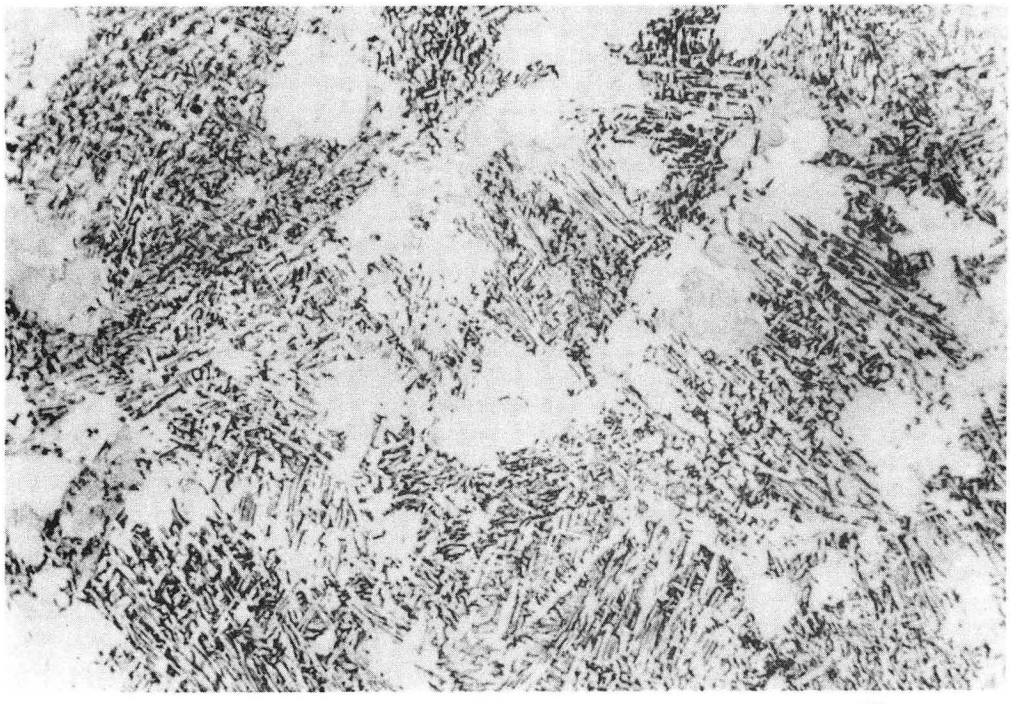

(b)

20μm

XBB 7210-5526

Fig. 15. Optical micrographs of 900°C (2 hrs) AQ + 700°C (0.5 hrs) IBQ heat treatment.

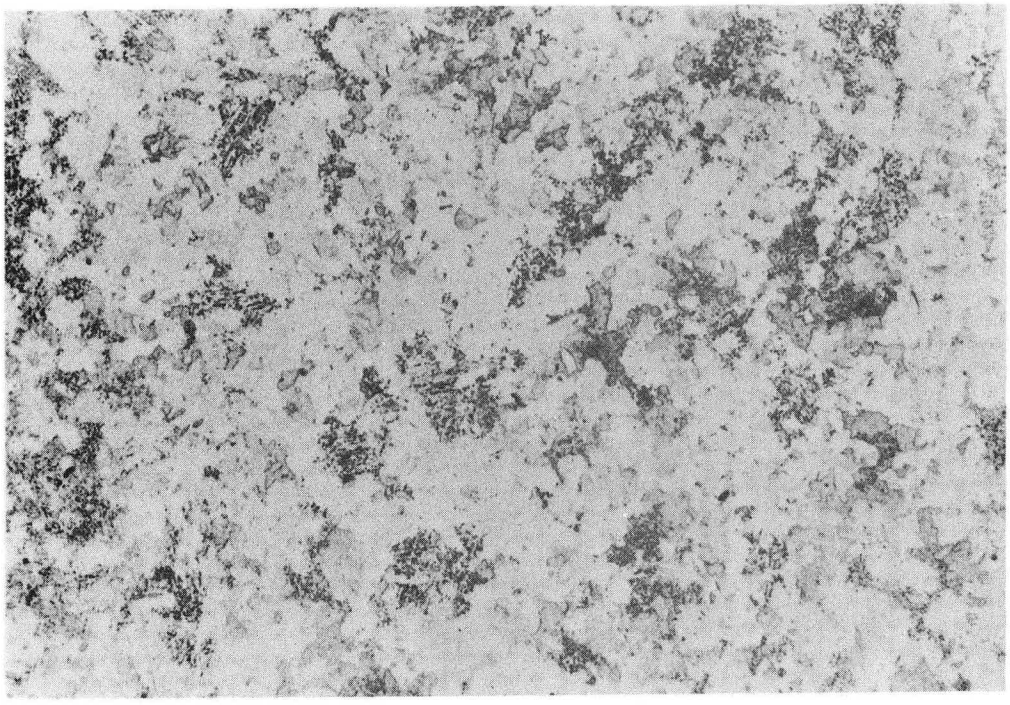

(a) 100μm

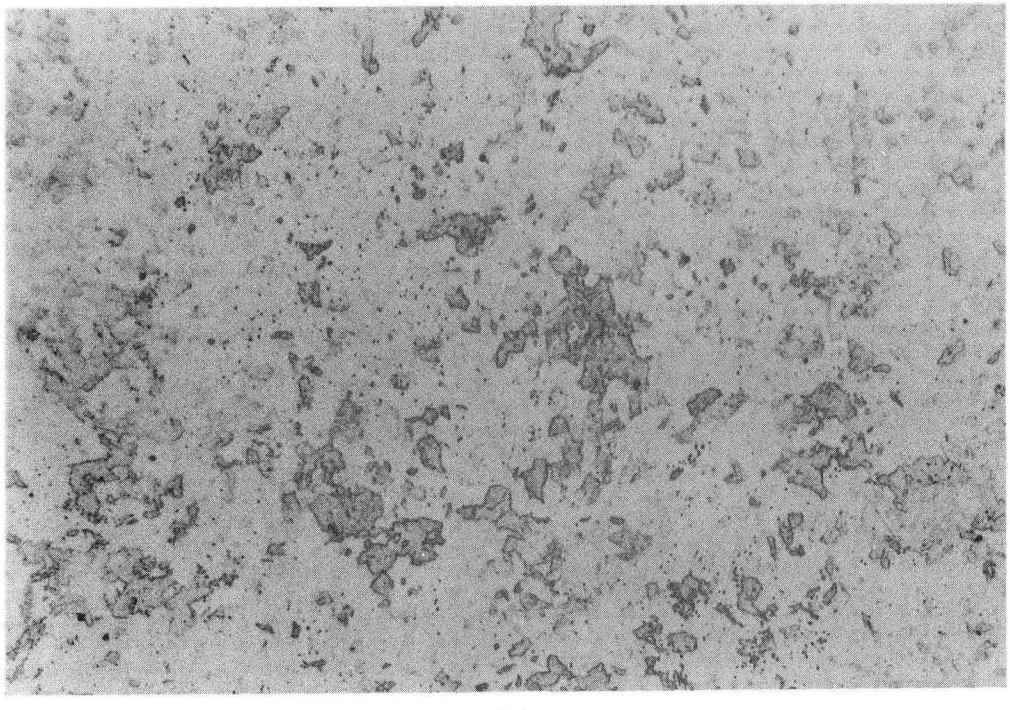

(b) XBB 7210-5523

Fig. 16. Optical micrographs of 900°C (2 hrs) AQ + (a) 700°C (1 hr) IBQ and (b) 700°C (6 hrs) IBQ heat treatments.

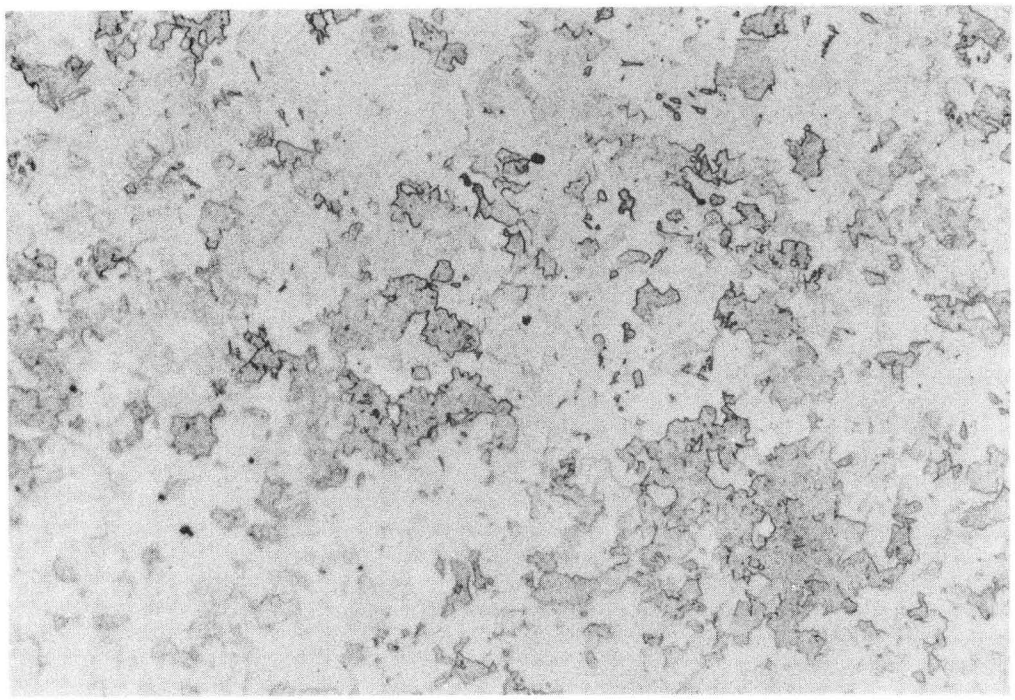

(a)

100μ

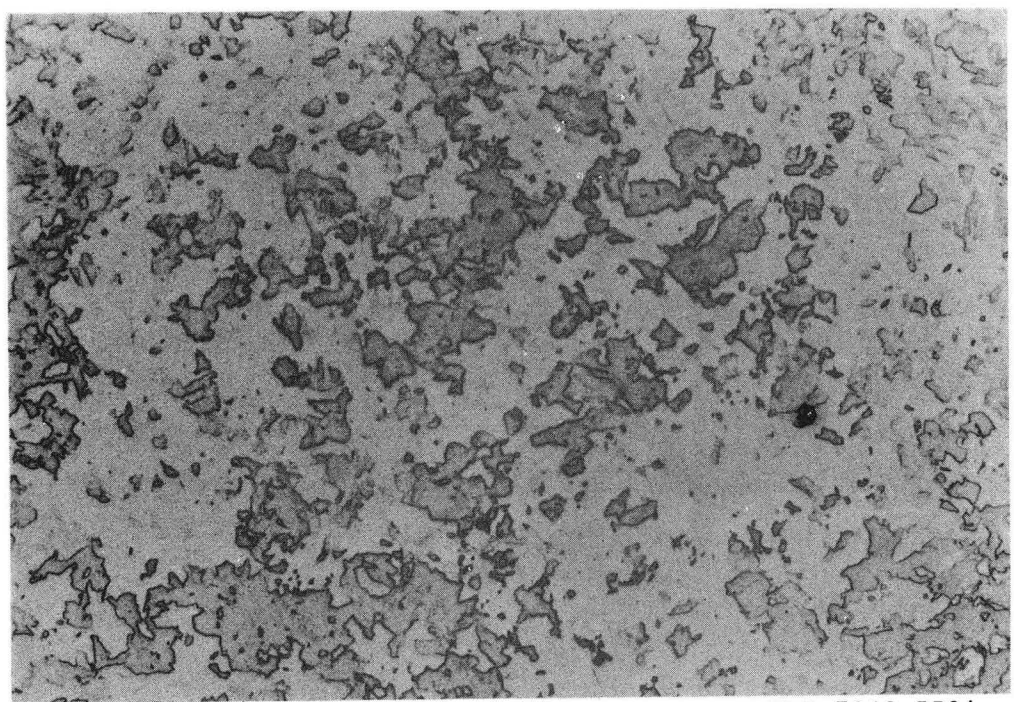

(b)

XBB 7210-5524

Fig. 17. Optical micrographs of 900°C (2 hrs) AQ + (a) 750°C (0.5 hrs) IBQ and (b) 750°C (2 hrs) IBQ heat treatments.

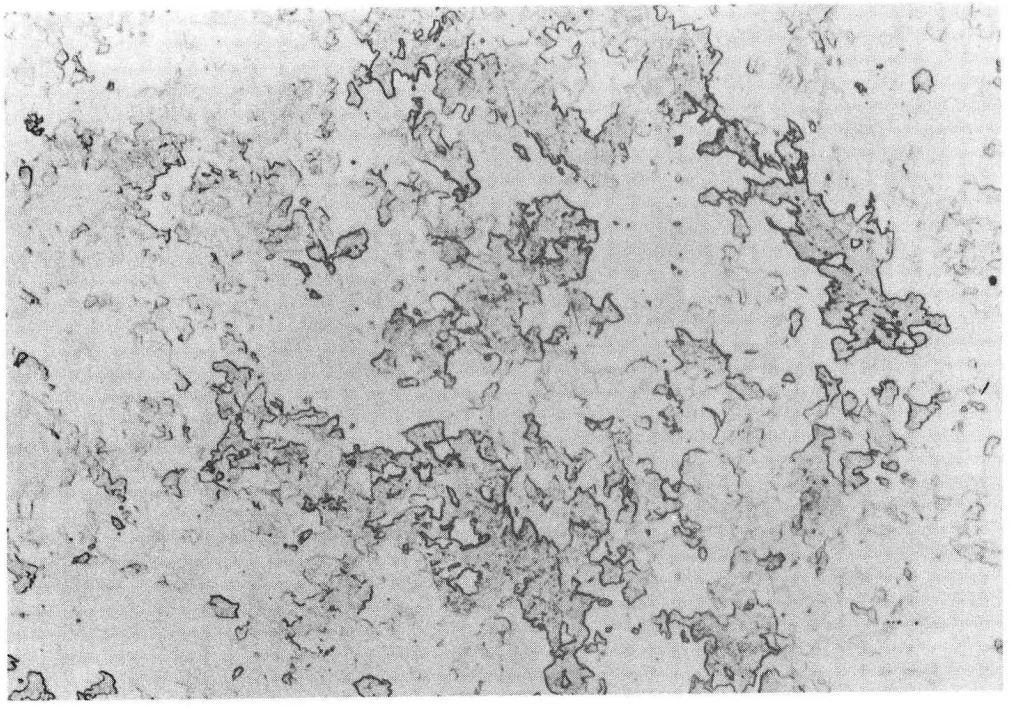

(a) 100μm

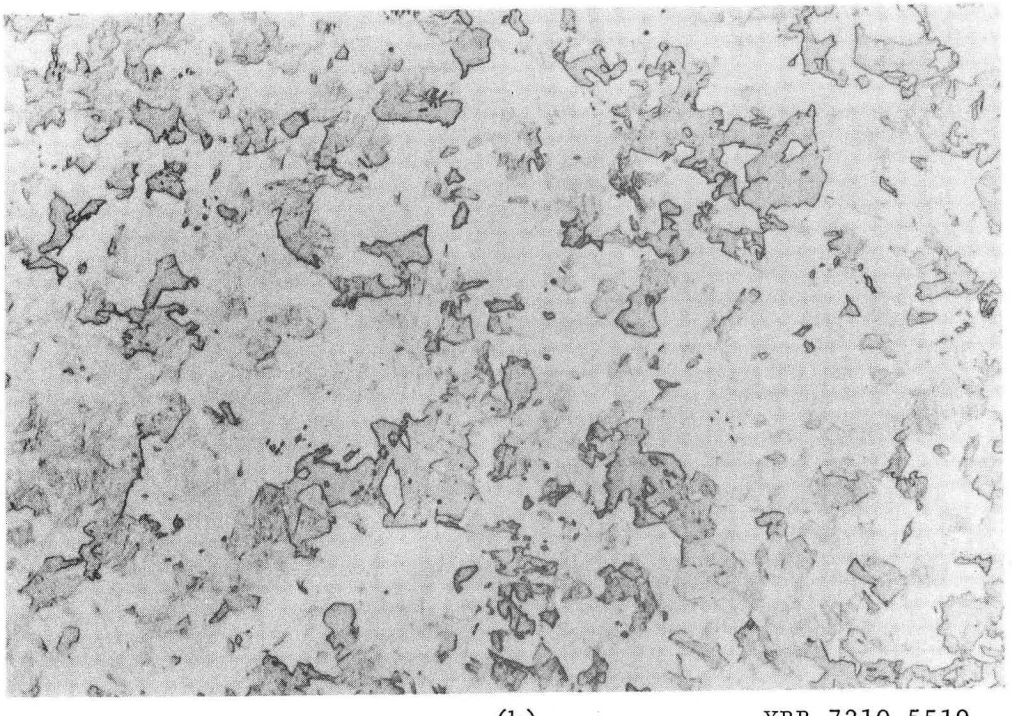

(b) XBB 7210-5519

Fig. 18. Optical micrographs of 900°C (2 hrs) AQ + (a) 800°C (0.2 hrs) IBQ and (b) 800°C (2 hrs) IBQ heat treatments.

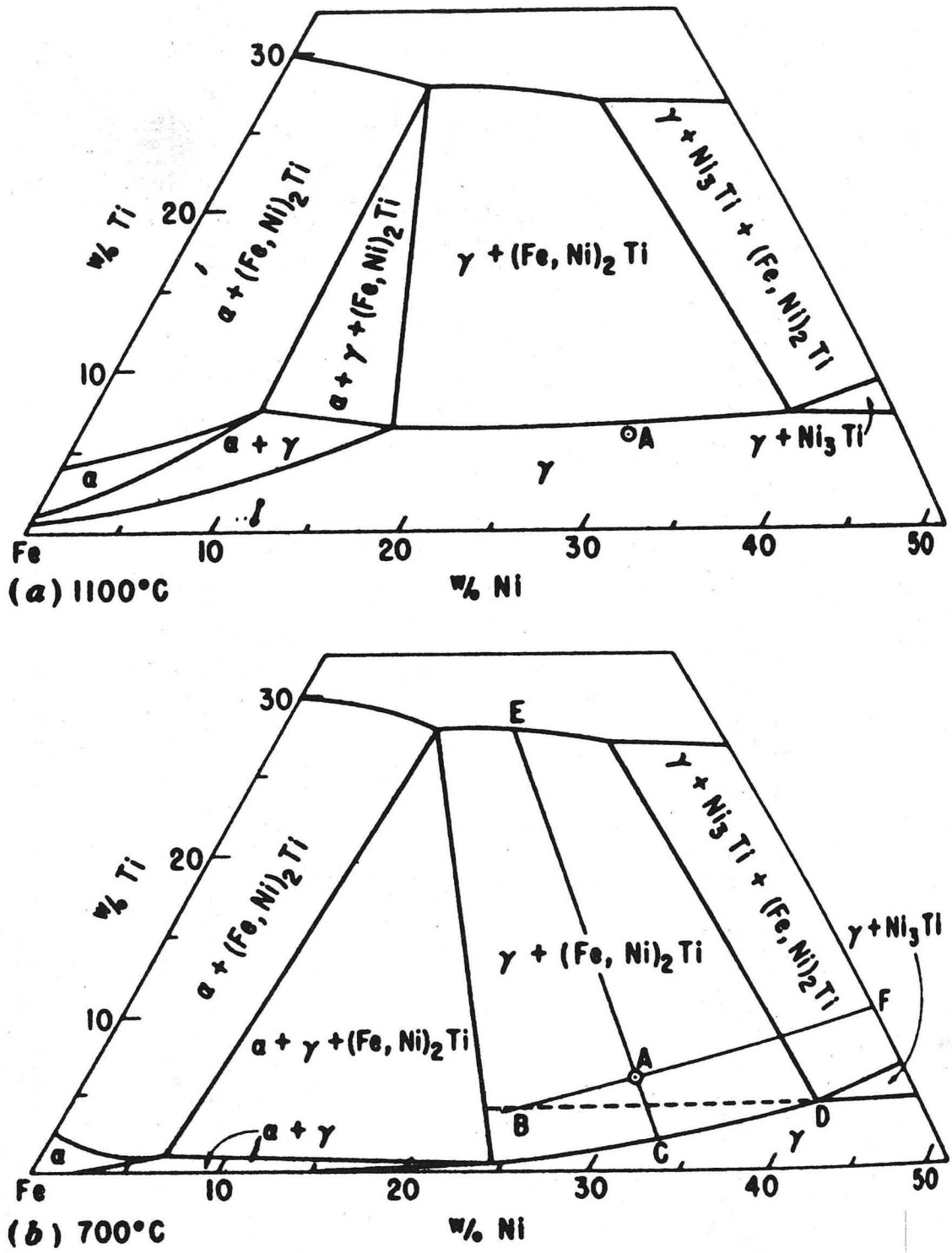

XBL 7210-5825

Fig. 19. Iron rich corner of ternary Fe-Ni-Ti equilibrium phase diagram (from Speich[22]).

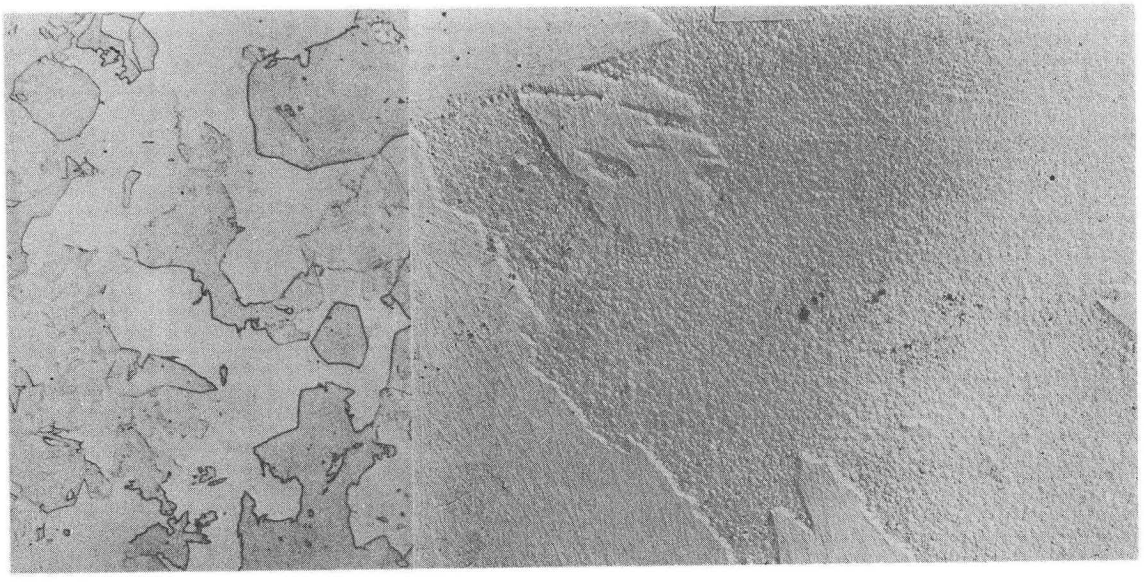

(a) 100μ (b) 5μ

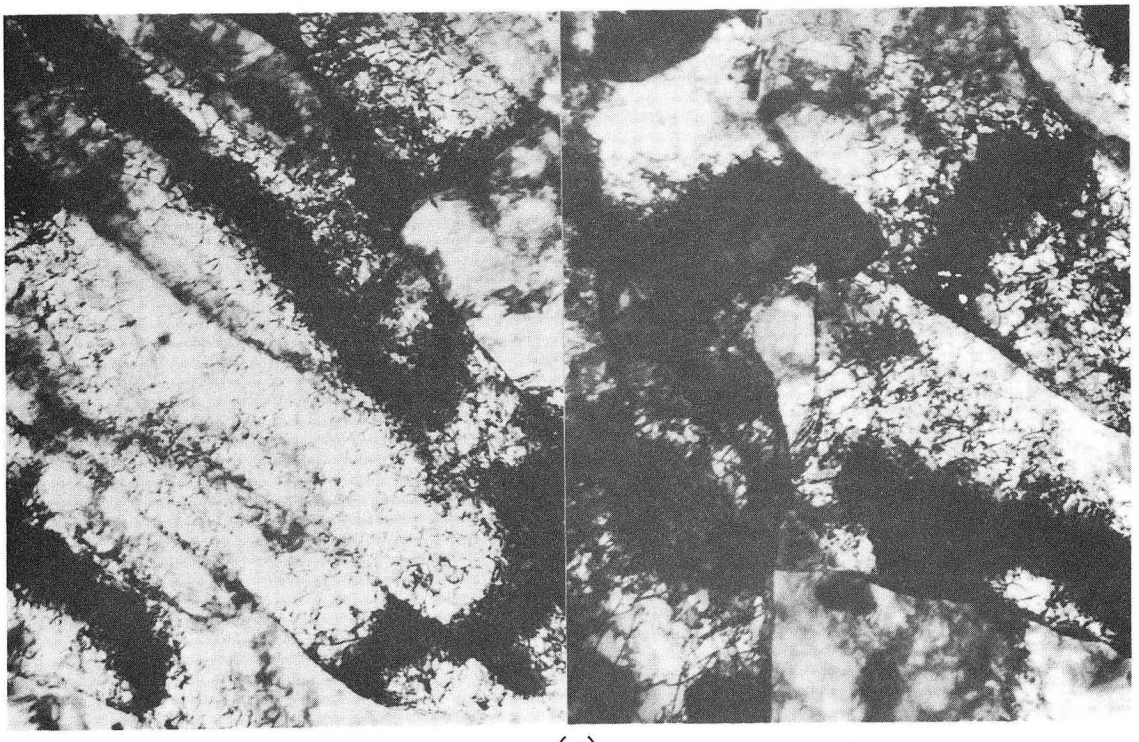

(c) 0.5μ

XBB 727-3819

Fig. 20. (a) Optical, (b) transmission replica and (c) transmission thin foil micrographs of 900°C (2 hrs) AQ heat treatment.

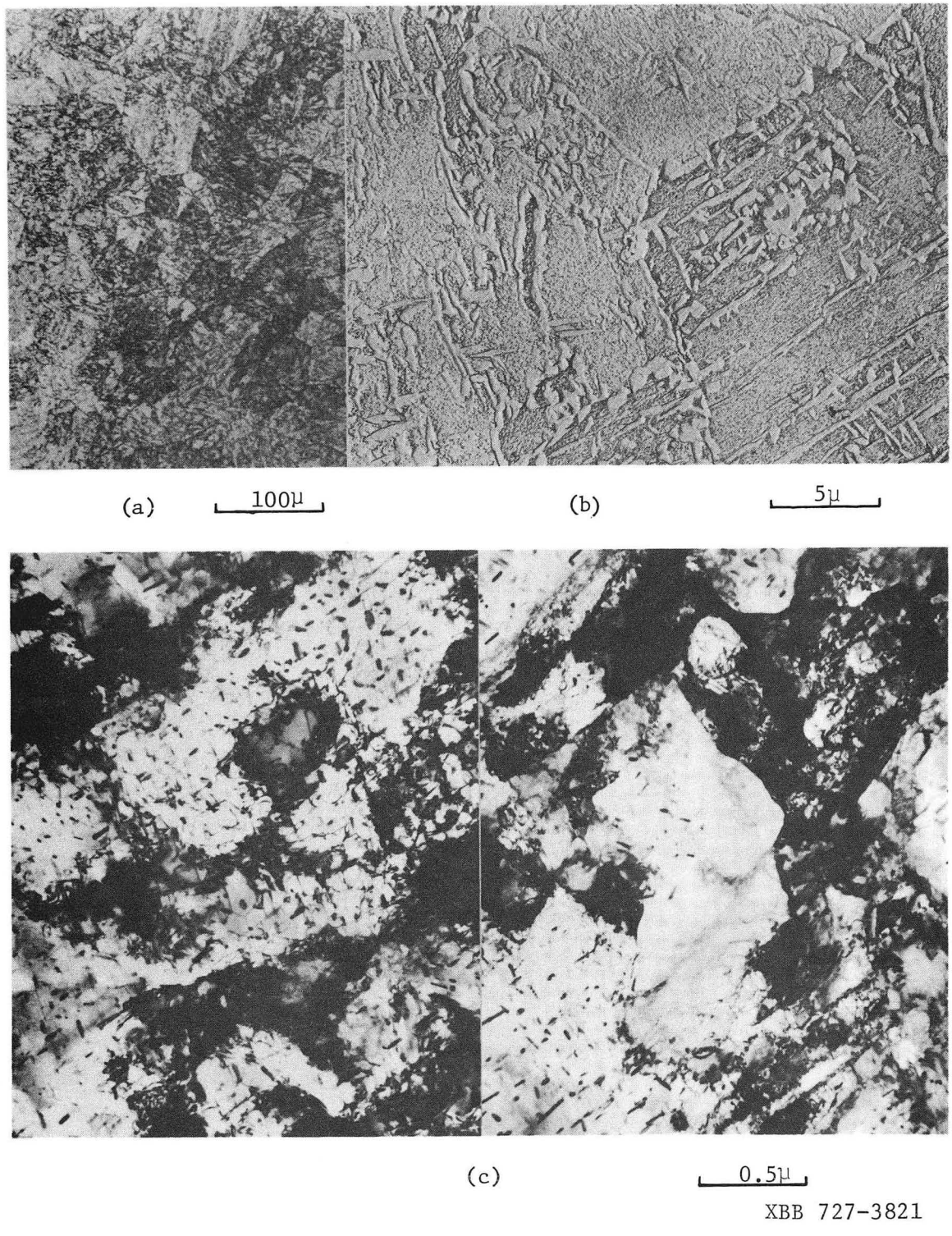

Fig. 21. (a) Optical, (b) transmission replica and (c) transmission thin foil micrographs of 900°C (2 hrs) AQ + 650°C (2 hrs) IBQ heat treatment.

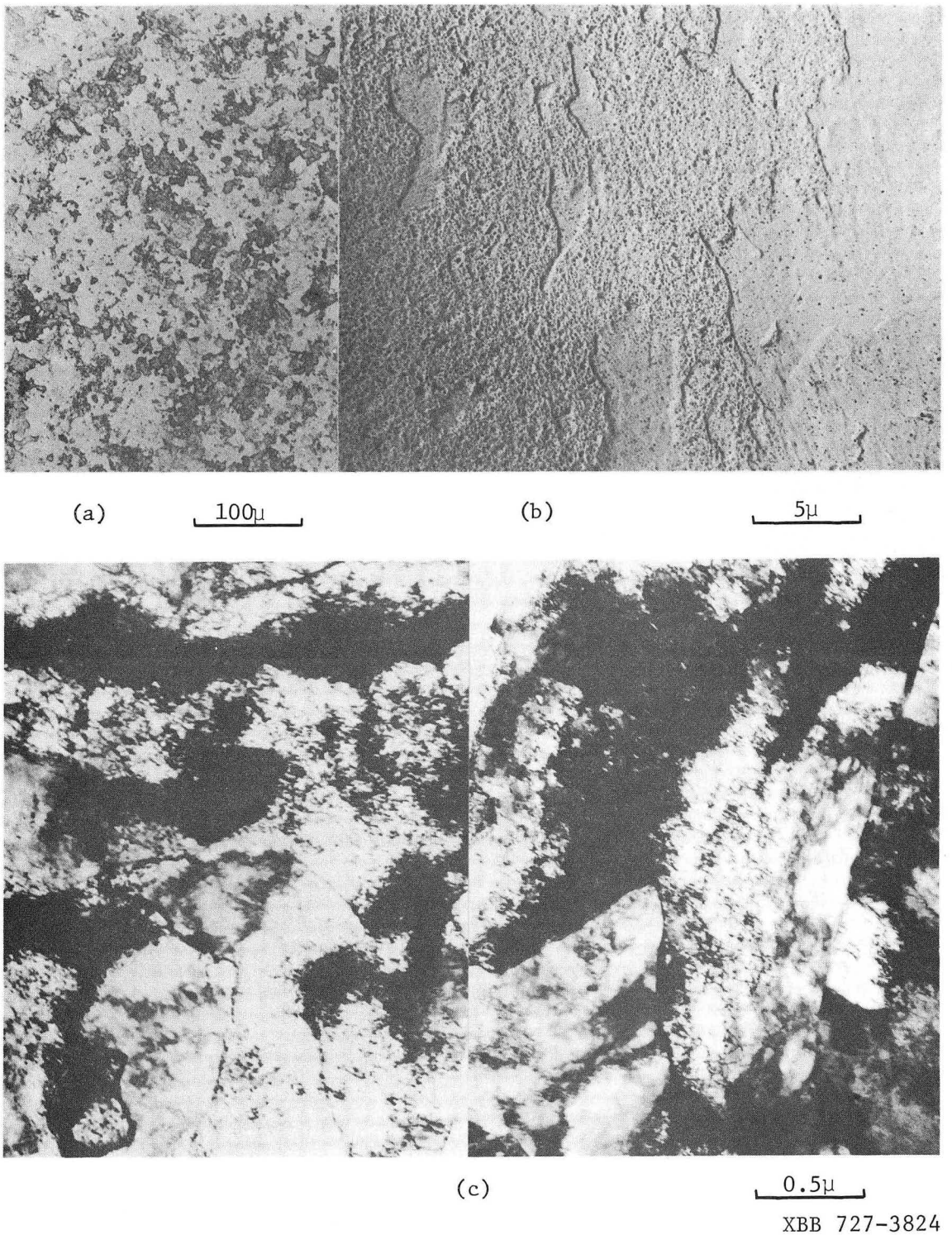

Fig. 22. (a) Optical, (b) transmission replica and (c) transmission thin foil micrographs of 900°C (2 hrs) AQ + 700°C (2 hrs) IBQ heat treatment.

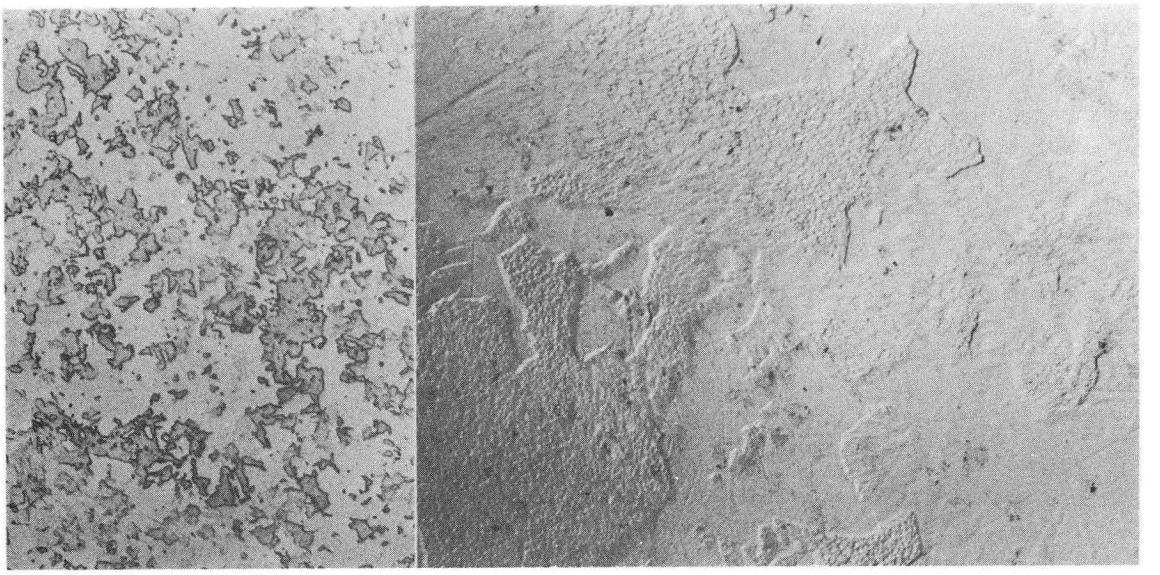

(a) 100μ (b) 5μ

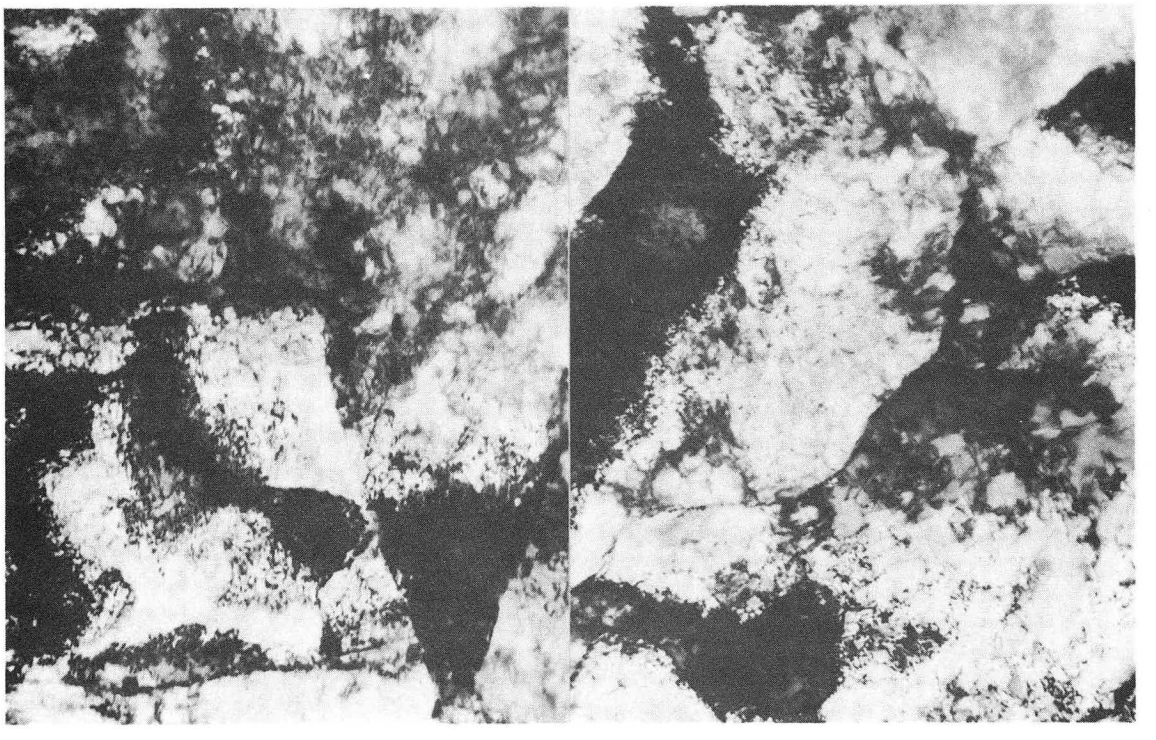

(c) 0.5μ

XBB 727-3822

Fig. 23. (a) Optical, (b) transmission replica and (c) transmission thin foil micrographs of 900°C (2 hrs) AQ + 750°C (2 hrs) IBQ heat treatment.

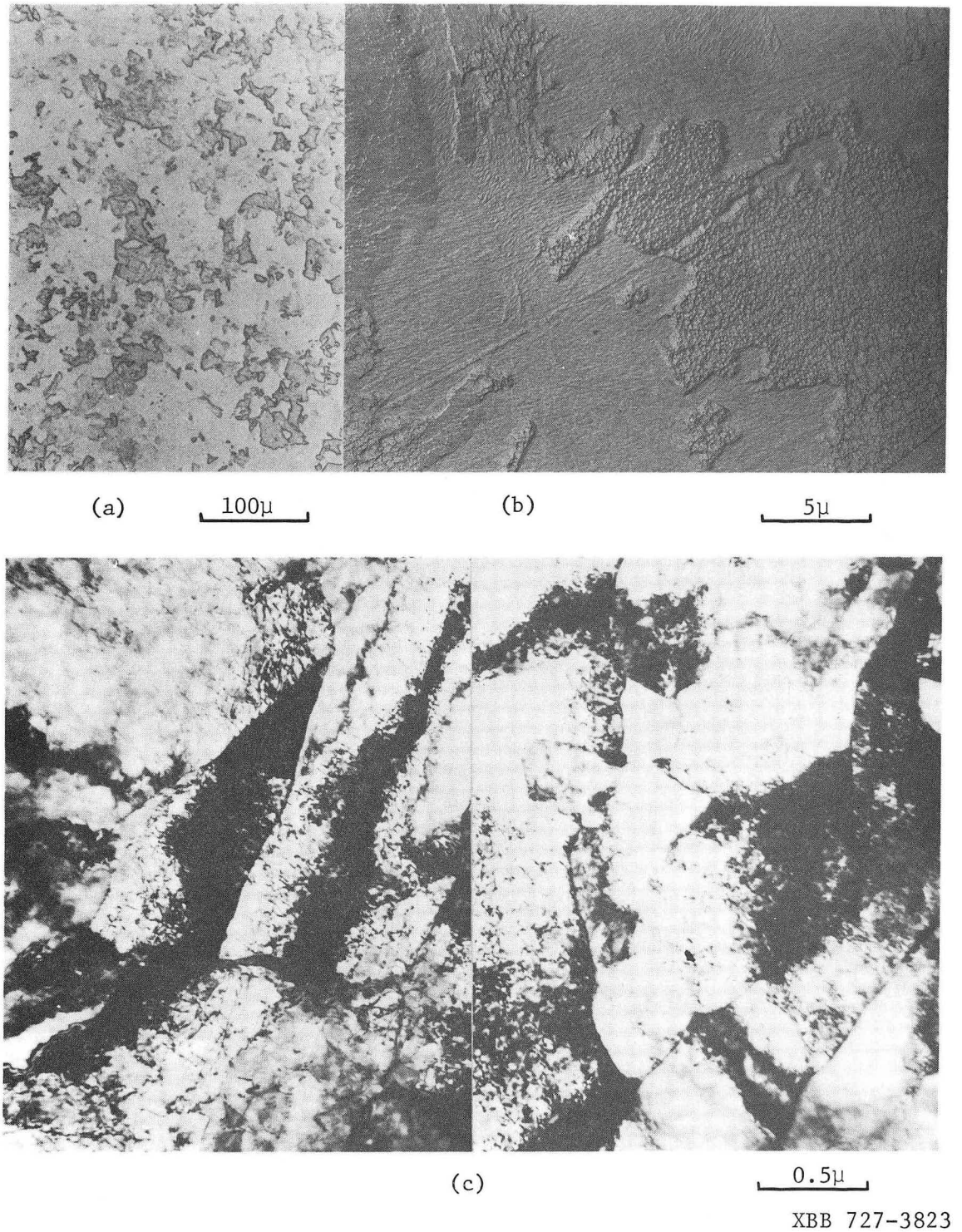

Fig. 24. (a) Optical, (b) transmission replica and (c) transmission thin foil micrographs of 900°C (2 hrs) AQ + 800°C (2 hrs) IBQ heat treatment.

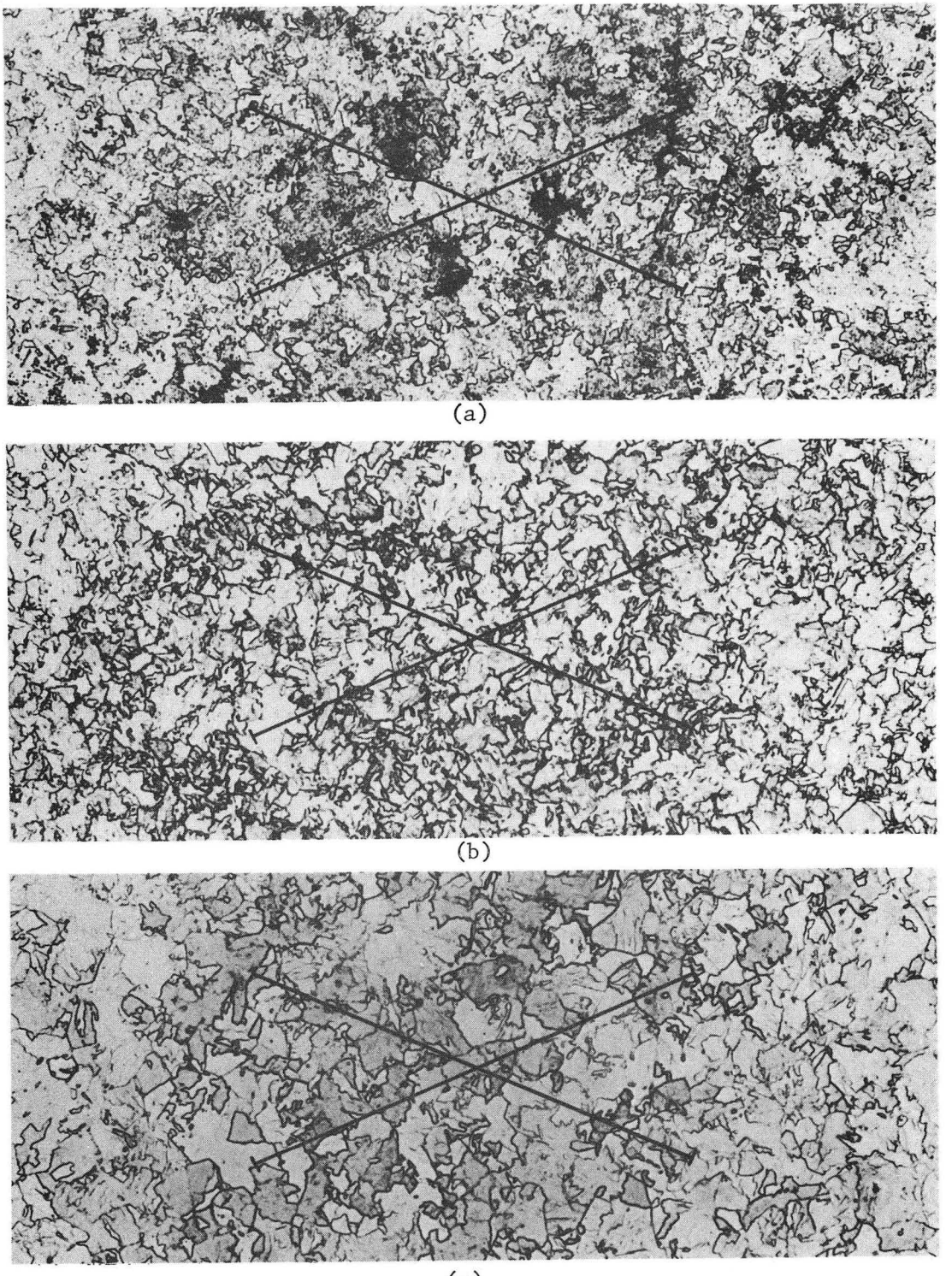

Fig. 25. Grain size determination of (a) 900°C(2 hrs)AQ + 700°C(2 hrs)AQ, (b) 900°C(2 hrs)AQ + 750°C(2 hrs)AQ and (c) 900°C(2 hrs)AQ + 800°C (2 hrs)AQ heat treatments. Lines represent 0.01 inch.

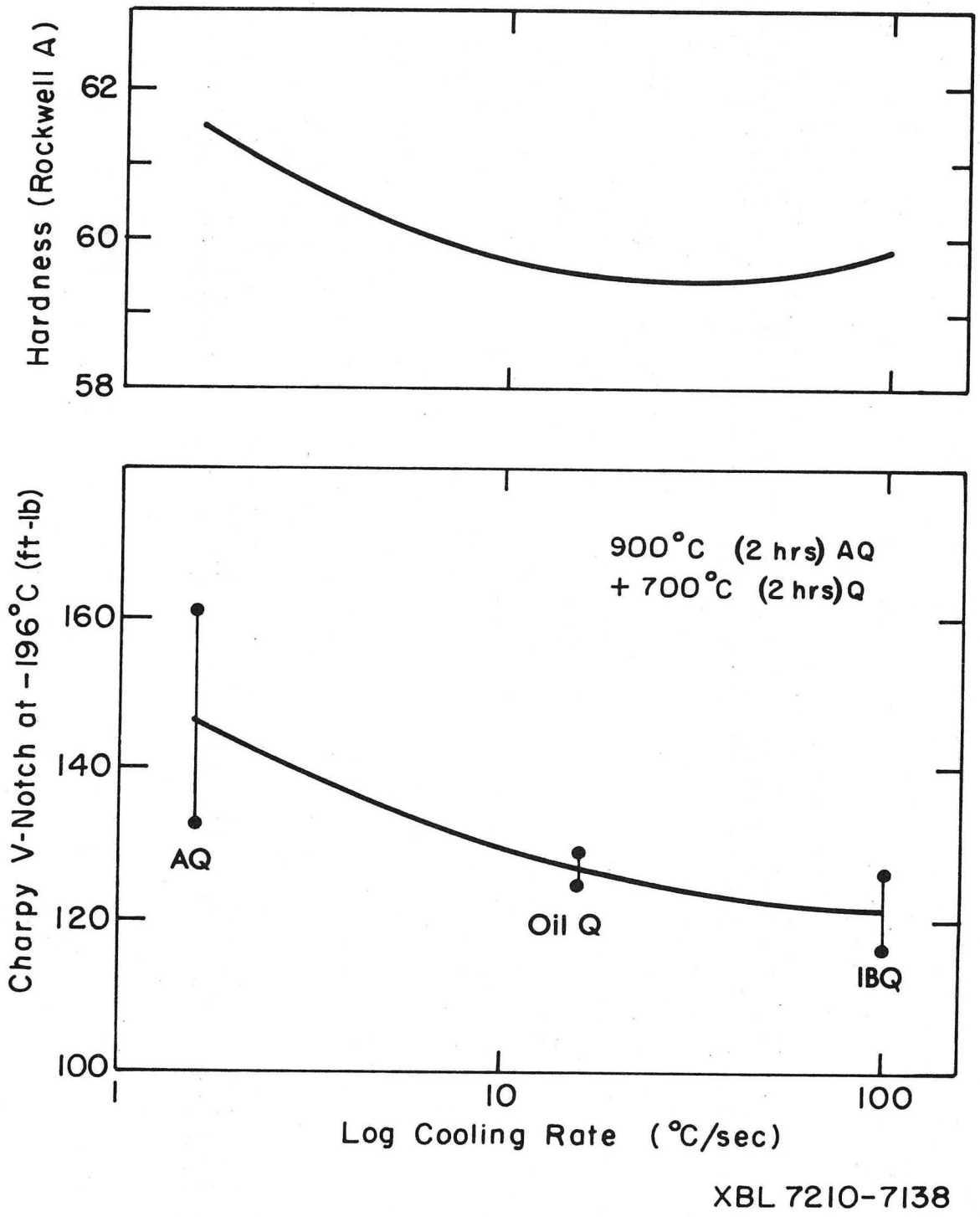

Fig. 26. Charpy impact energy at -196°C and hardness vs log cooling rate for the 900°C(2 hrs)AQ + 700°C(2 hrs)Q condition.

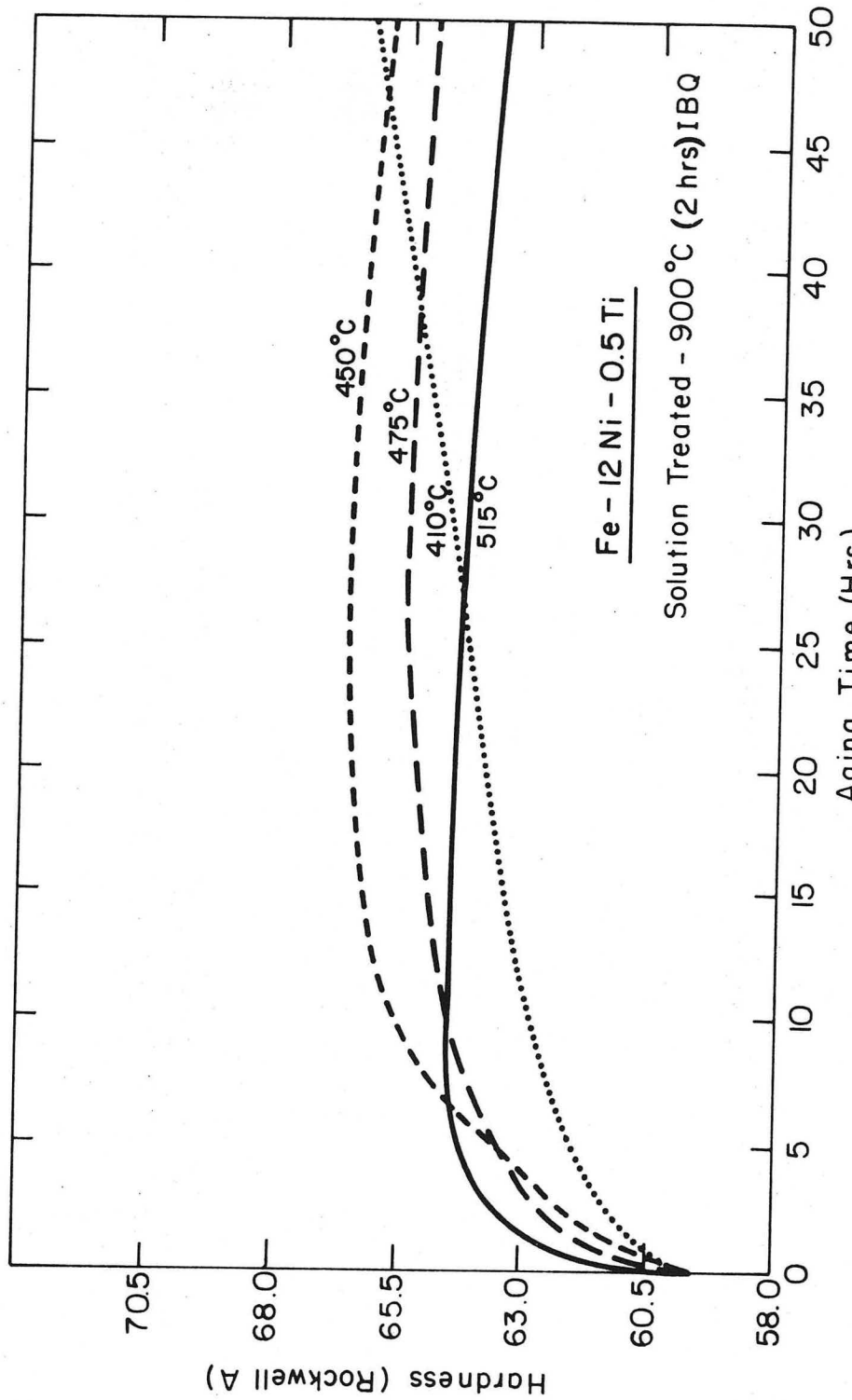

XBL729-6979

Fig. 27. Hardness vs isothermal aging of four temperatures from the 900°C(2 hrs) IBQ condition.

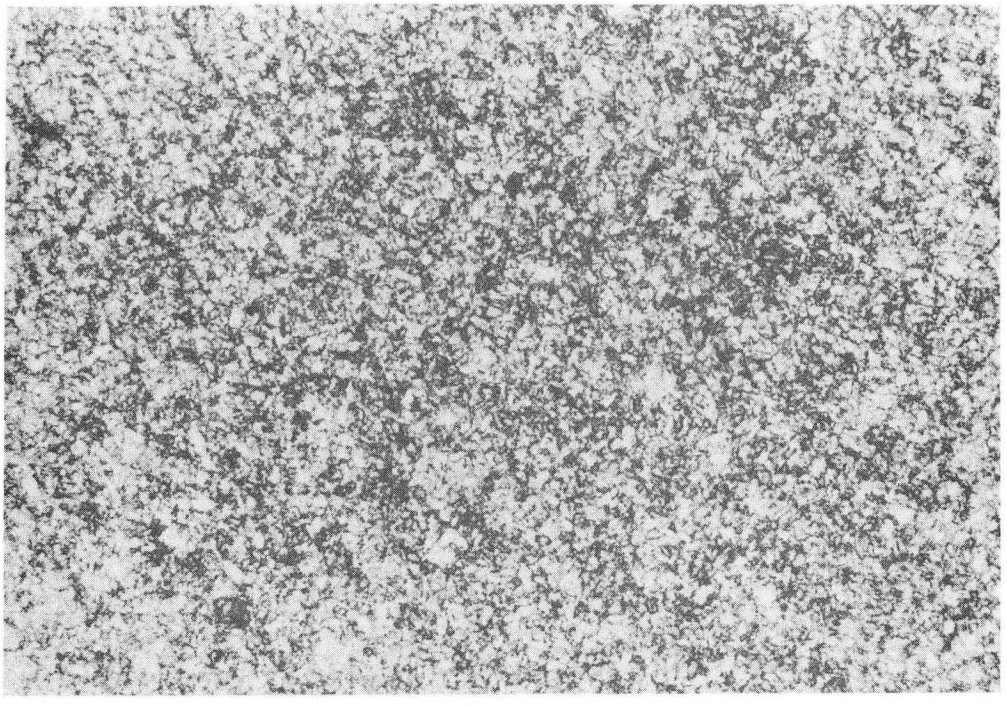

(a)

100μ

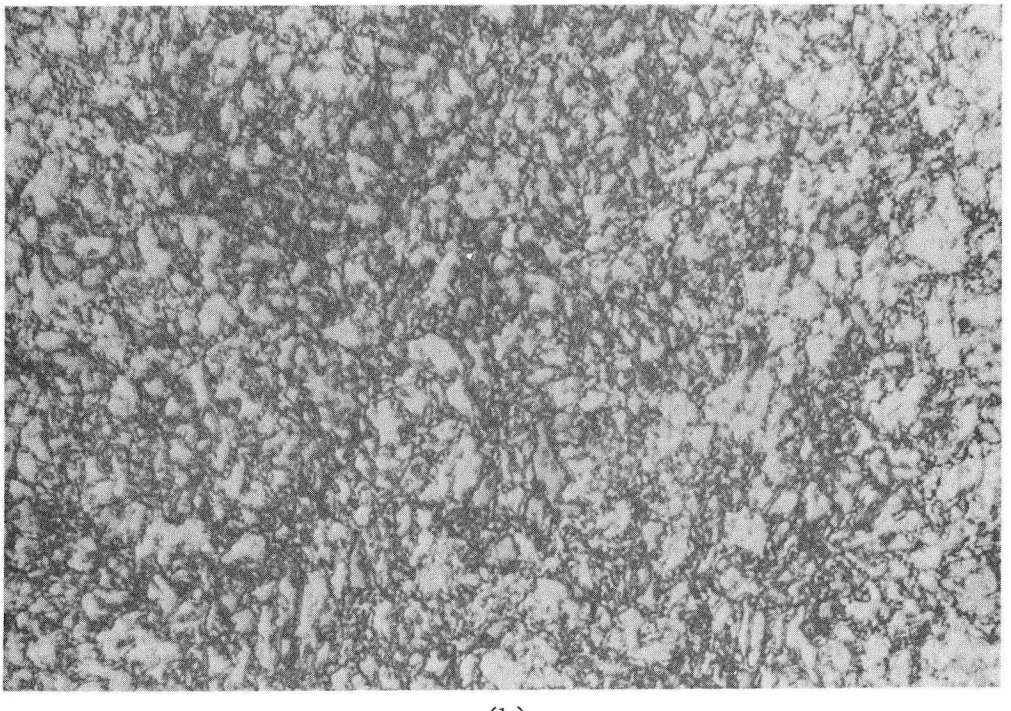

(b)

20μ

XBB 7210-5529

Fig. 28. Optical micrographs of as forged + 650°C (2 hrs) IBQ heat treatment.

XBB 7211-5847

Fig. 29. Replica Transmission electron micrograph of as forged + 650°C (2 hrs) IBQ structure.

XBB 727-3820

Fig. 30. Transmission thin foil micrograph of as forged + 650°C (2 hrs) IBQ heat treatment.

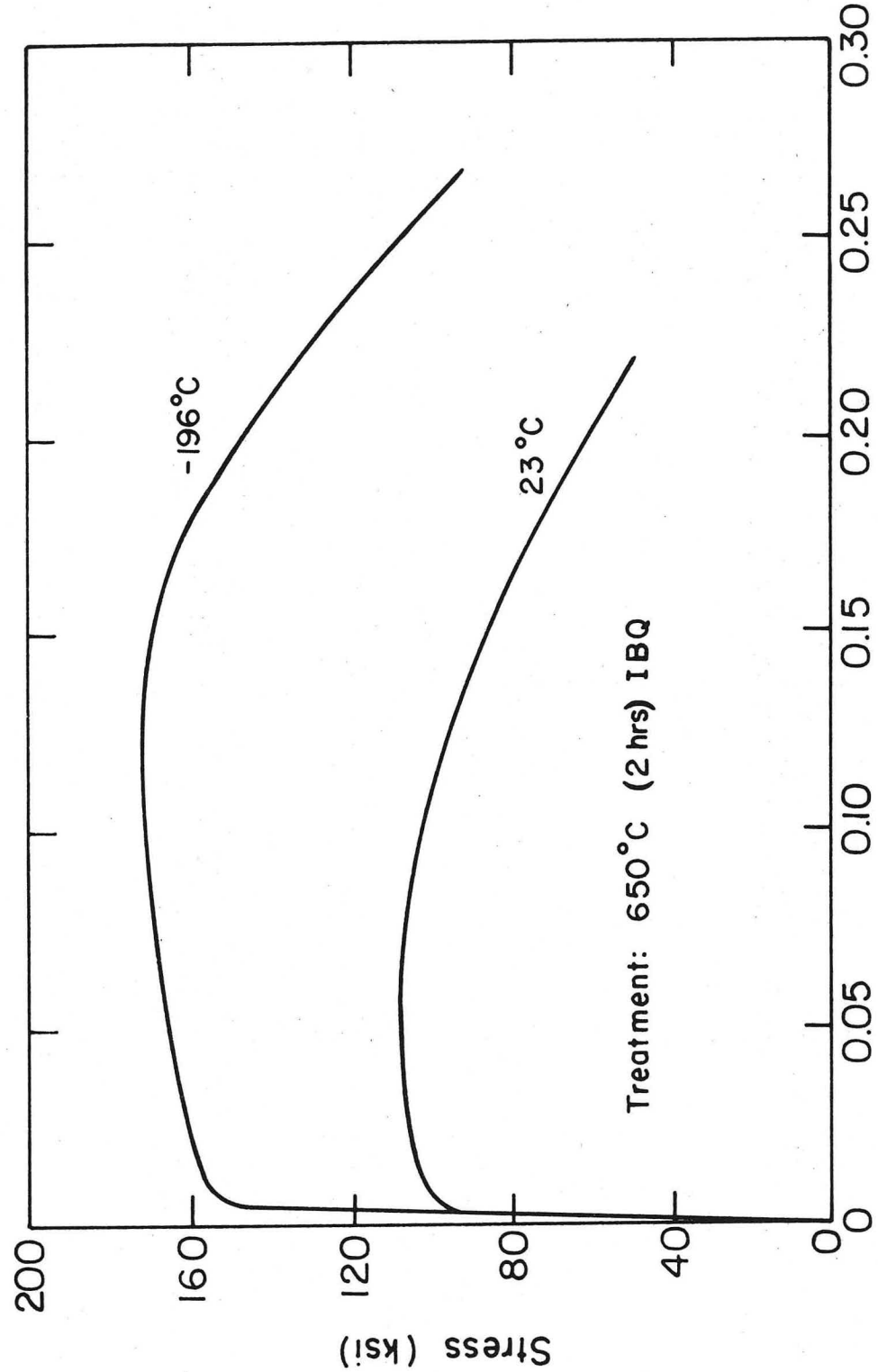

Fig. 31. Stress-strain curves at 23°C and -196°C for the as forged + 650°C(2 hrs)IBQ condition.

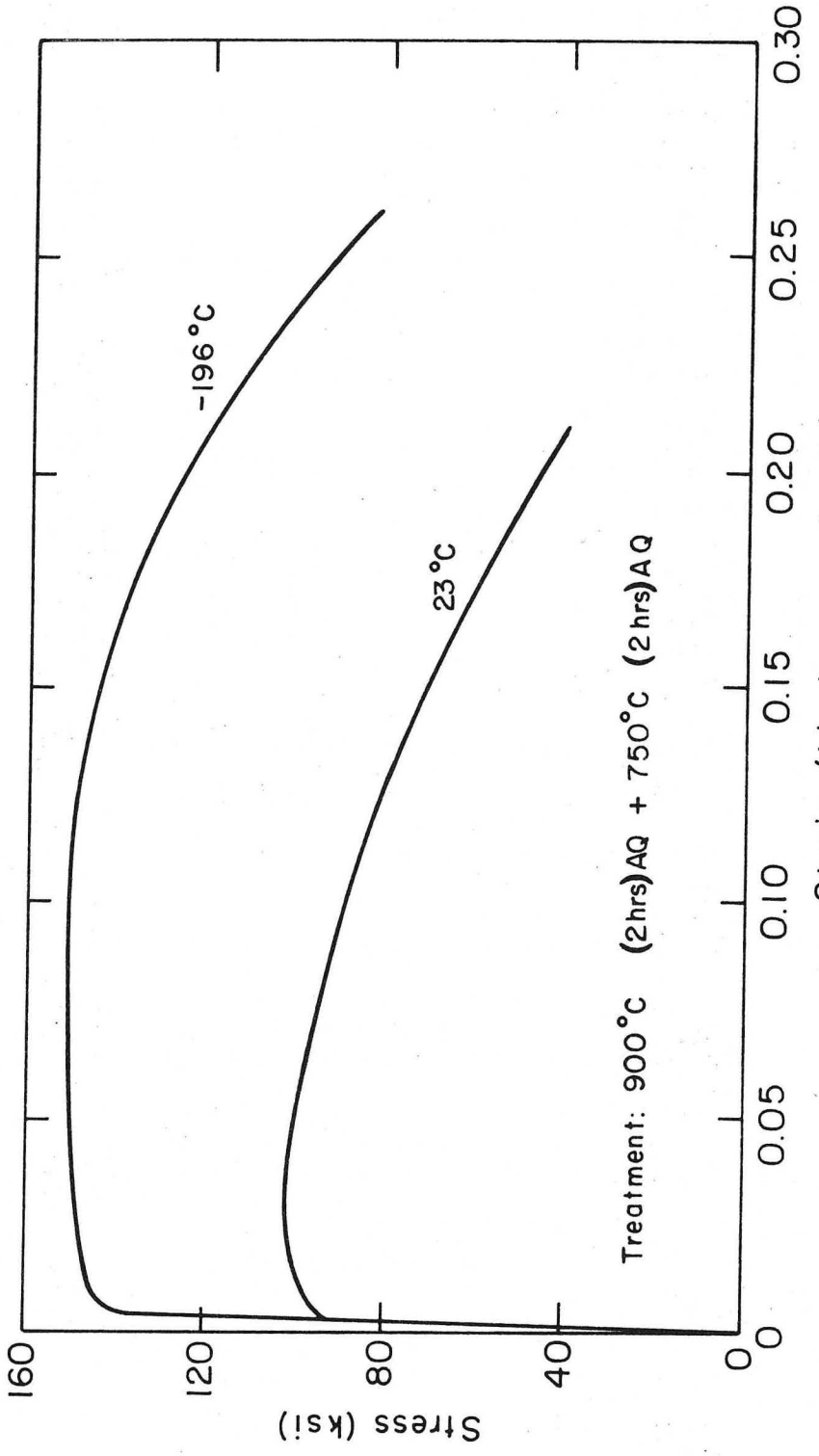

Fig. 32. Stress-strain curves at 23°C and -196°C for the 900°C 2 hrs AQ + 750°C(2 hrs)AQ condition

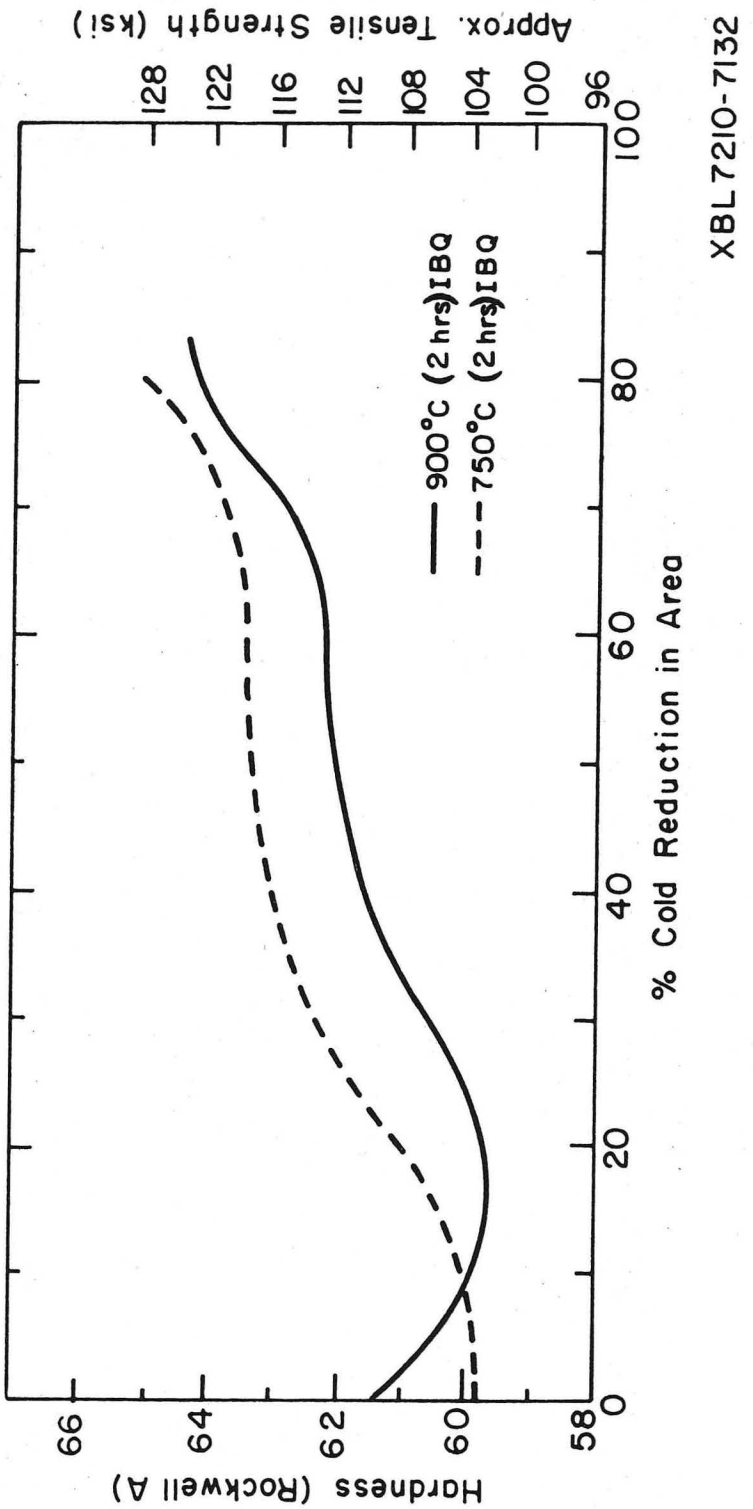

Fig. 33. Hardness and approximate tensile strength vs % cold reduction for two heat treatments.

APPENDIX. ADDITIONAL DATA ON THE Fe-12 wt% Ni-0 to 2 wt% Ti ALLOY SYSTEM FOR FUTURE REFERENCE

Alloy Compositions

Ingot #	726-12	722-10	708-15	7010-6
Ni (wt%)	11.96	12.35	12.06	12.02
Ti (wt%)	0.22	0.54	0.94	2.00

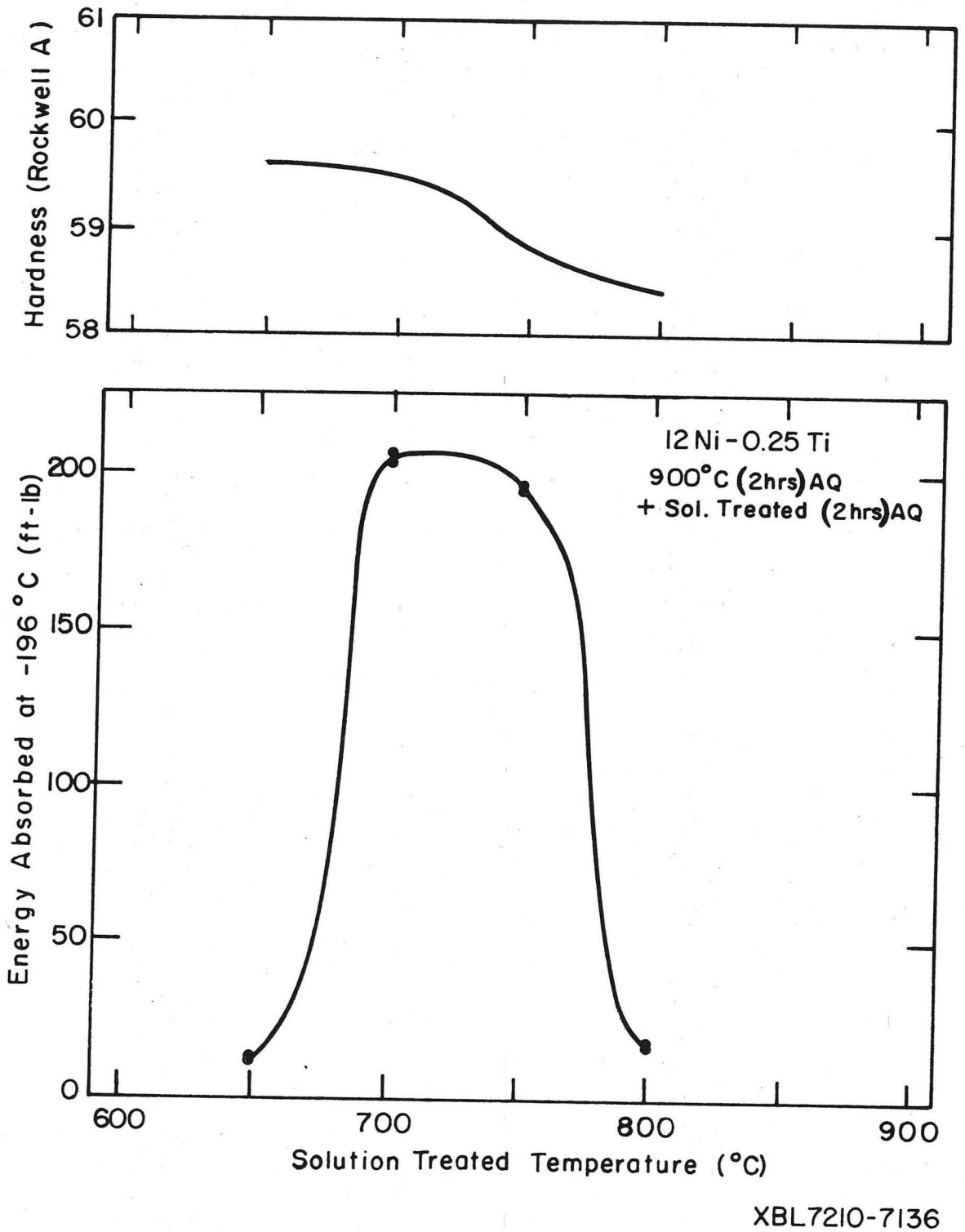

Charpy impact energy at -196°C and hardness vs temperature + AQ for the 900°C (2 hrs) AQ condition. Alloy: Fe-12 wt% Ni-0.25 wt% Ti.

Variation of tensile properties of Fe-12 wt% Ni-0.25 wt/% Ti alloy with temperature for 3 heat treatments.

		Heat Treatment		
		900°C(2 hrs)AQ +650°C(2 hrs)AQ	900°C(2 hrs)AQ + 750°C(2 hrs)AQ	900°C(2 hrs)AQ +850°C(2 hrs)AQ
23°C	Tensile Strength (psi)	105,000 psi	93,400 psi	93,400 psi
	0.2% Yield Strength (psi)	101,000 psi	86,500 psi	85,500 psi
	% Elongation*	25%	24%	25%
	% Red. Area	84%	88%	88%
-196°C	Tensile Strength (psi)	158,000 psi	146,000 psi	146,000 psi
	0.2% Yield Strength (psi)	148,000 psi	133,000 psi	133,500 psi
	% Elongation*	21%	29%	25%
	% Red. Area	71%	78%	75%

*1 inch gauge length by 0.250 inch diameter specimen.

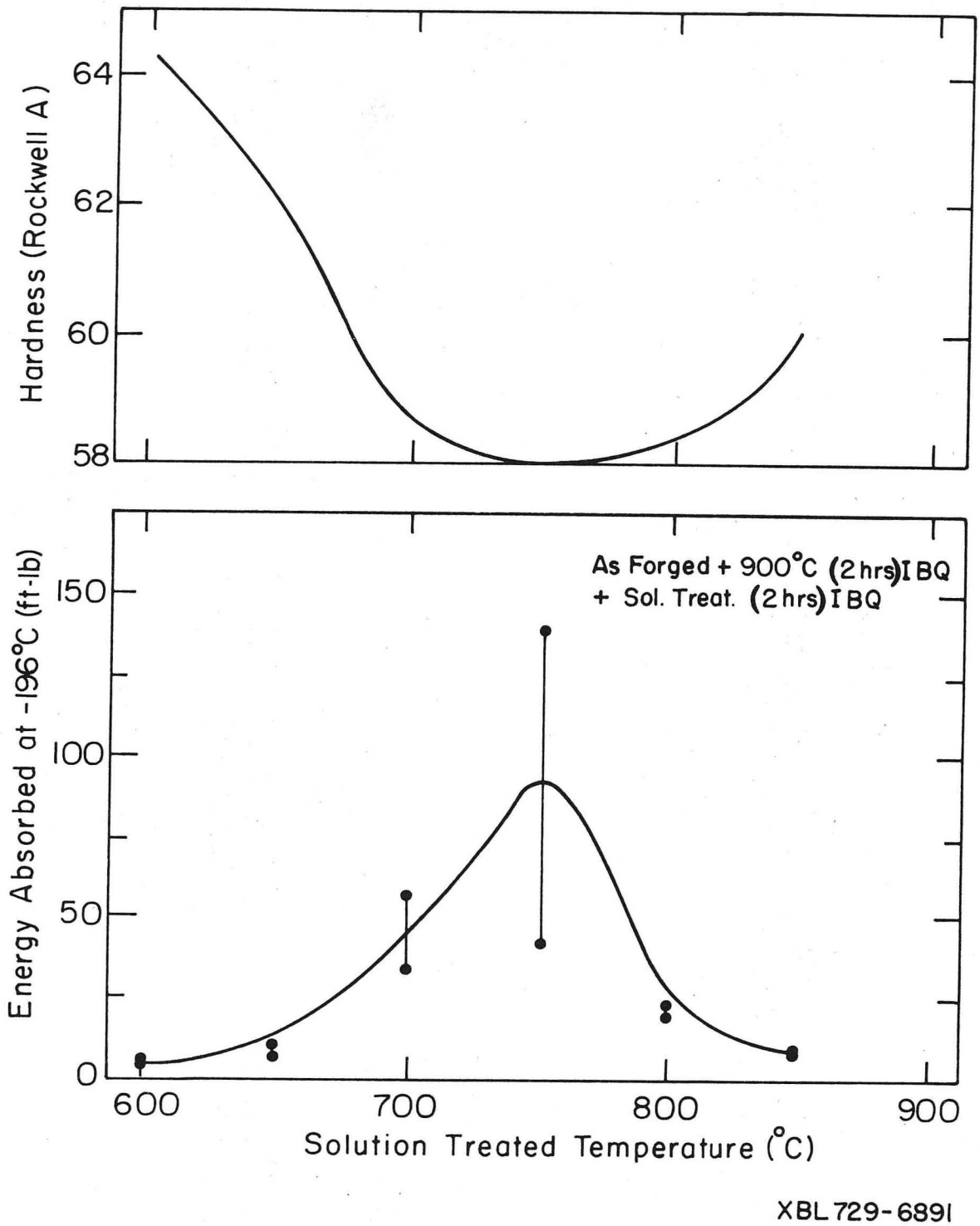

Charpy impact energy at -196°C and hardness vs temperature from the 900°C-2 hrs IBQ condition. Alloy: Fe-12 wt% Ni-0.5 wt% Ti.

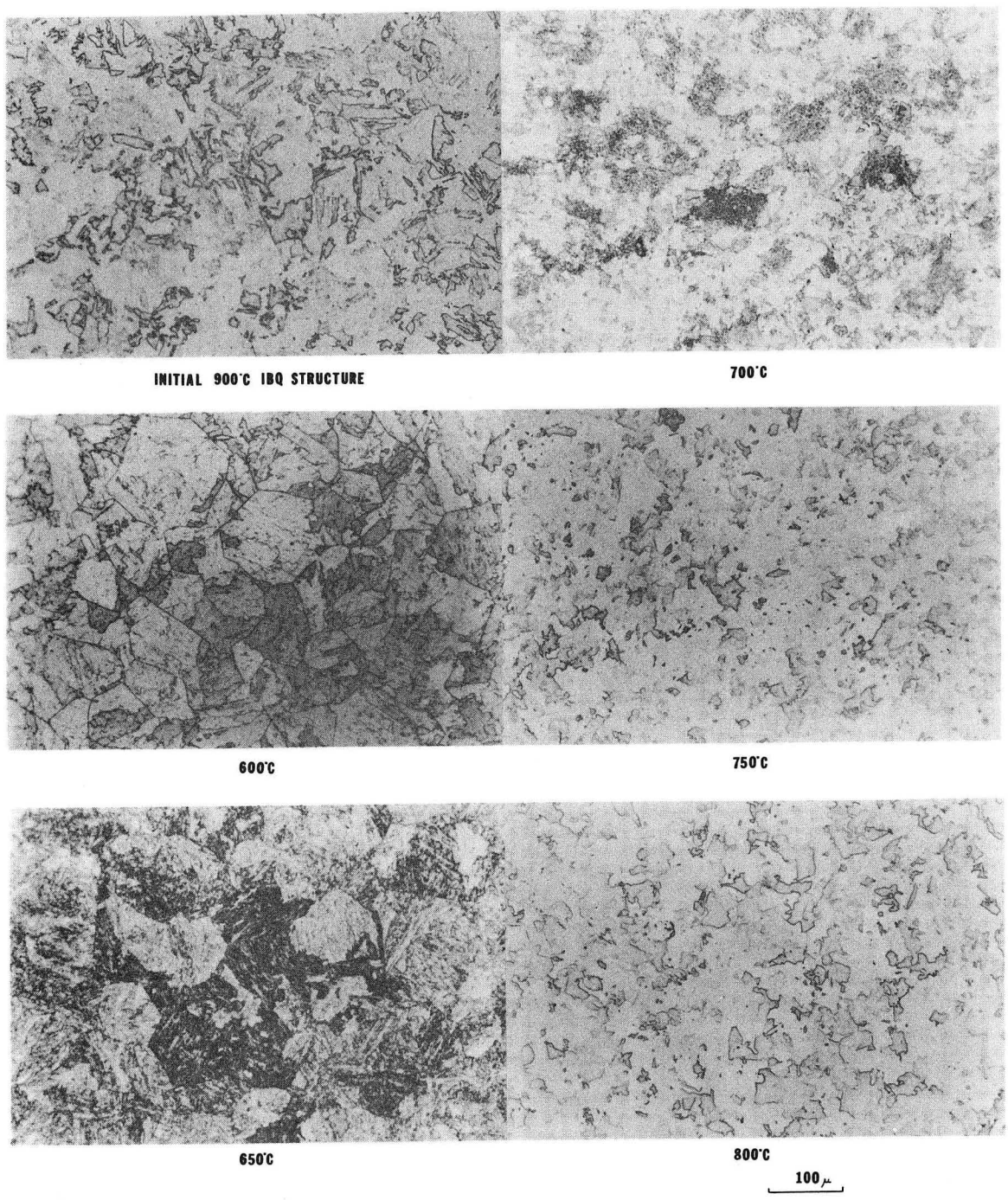

XBB 7210-5520

Optical micrographs of 900°C (2 hrs) IBQ + 600°C to 800°C (2 hrs) IBQ heat treatment. Alloy: Fe-12 wt% Ni-0.5wt% Ti.

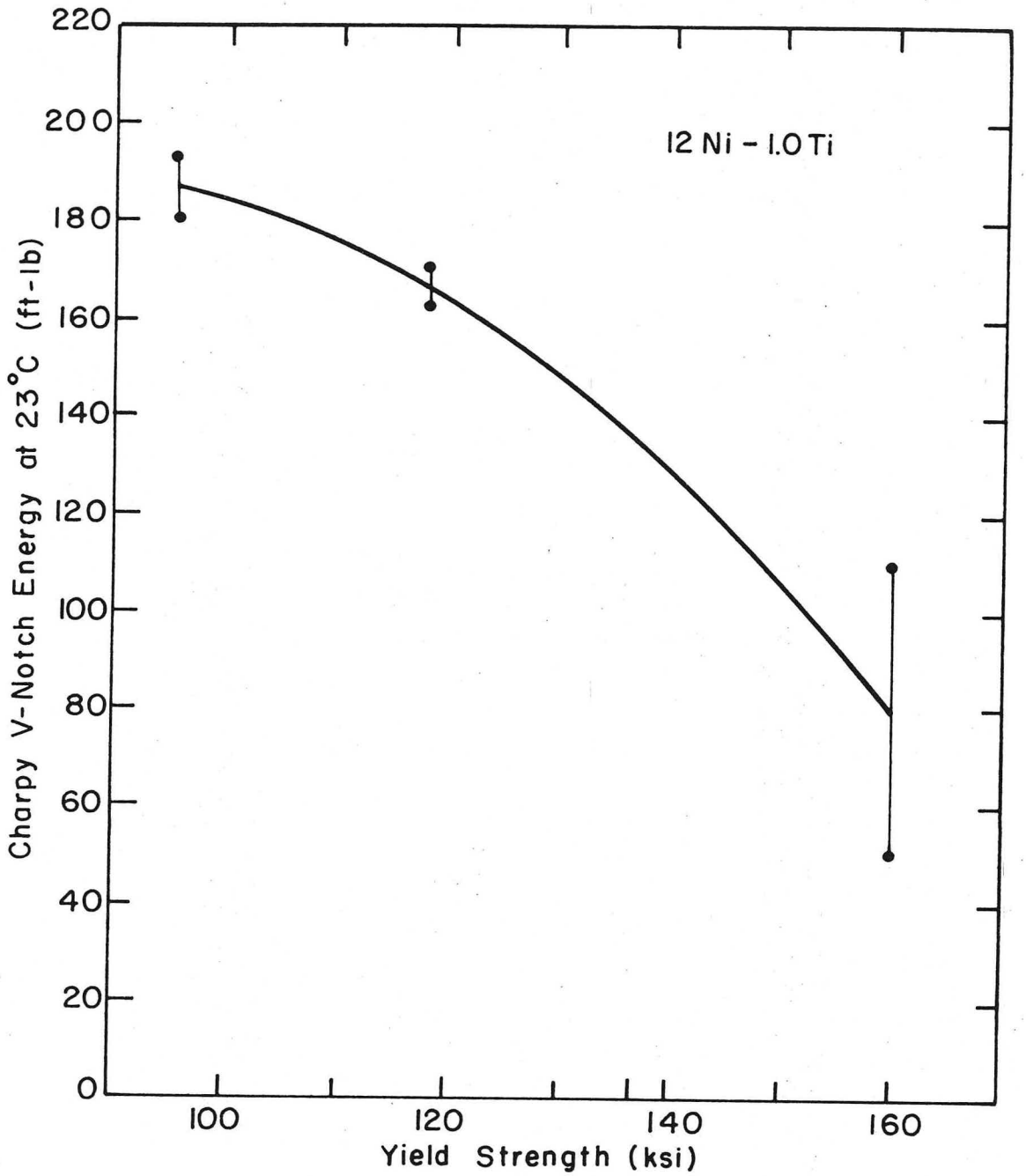

Room temperature Charpy impact energy vs yield strength as produced by isothermal aging at 475°C for 0 to 10 hrs. Alloy: Fe-12 wt% Ni-1.0 wt% Ti.

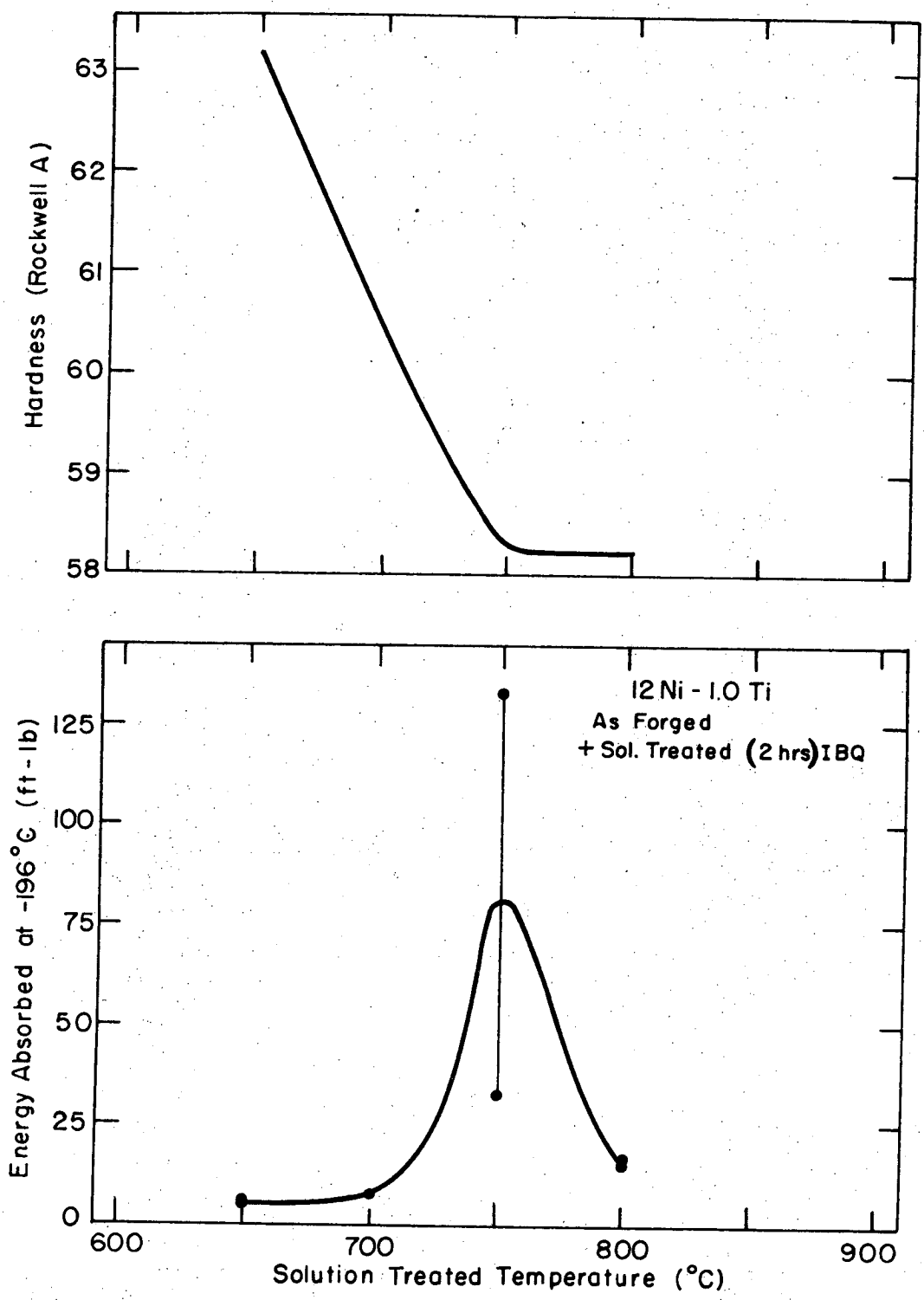

XBL 7210-7135

Charpy impact energy at -196°C and hardness vs temperature + IBQ from the as forged condition. Alloy Fe-12 wt% Ni-1.0 wt% Ti.

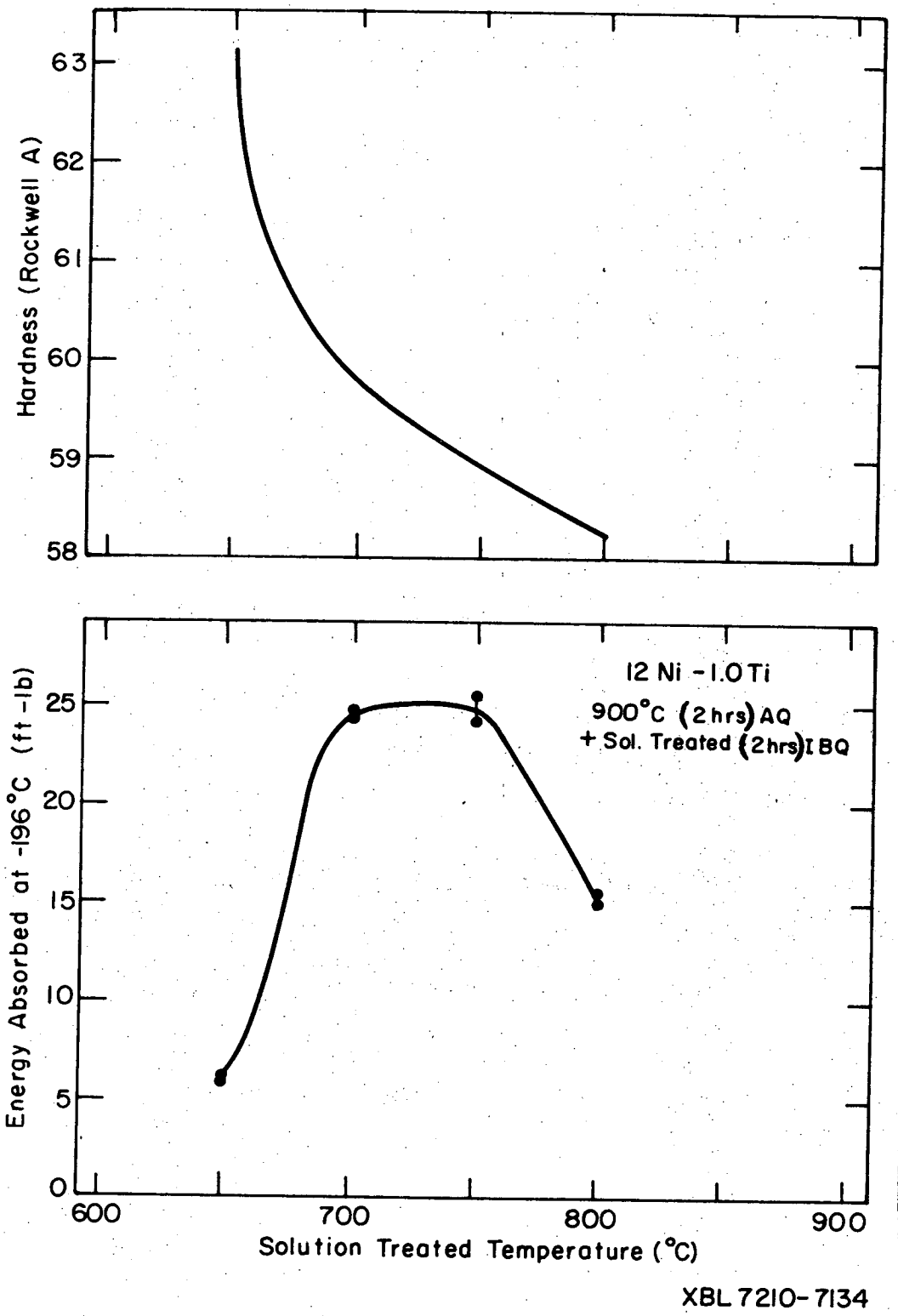

Charpy impact energy at -196°C and hardness vs temperature + IBQ from the 900°C (2 hrs) AQ condition. Alloy Fe-12 wt% Ni-1.0 wt% Ti.

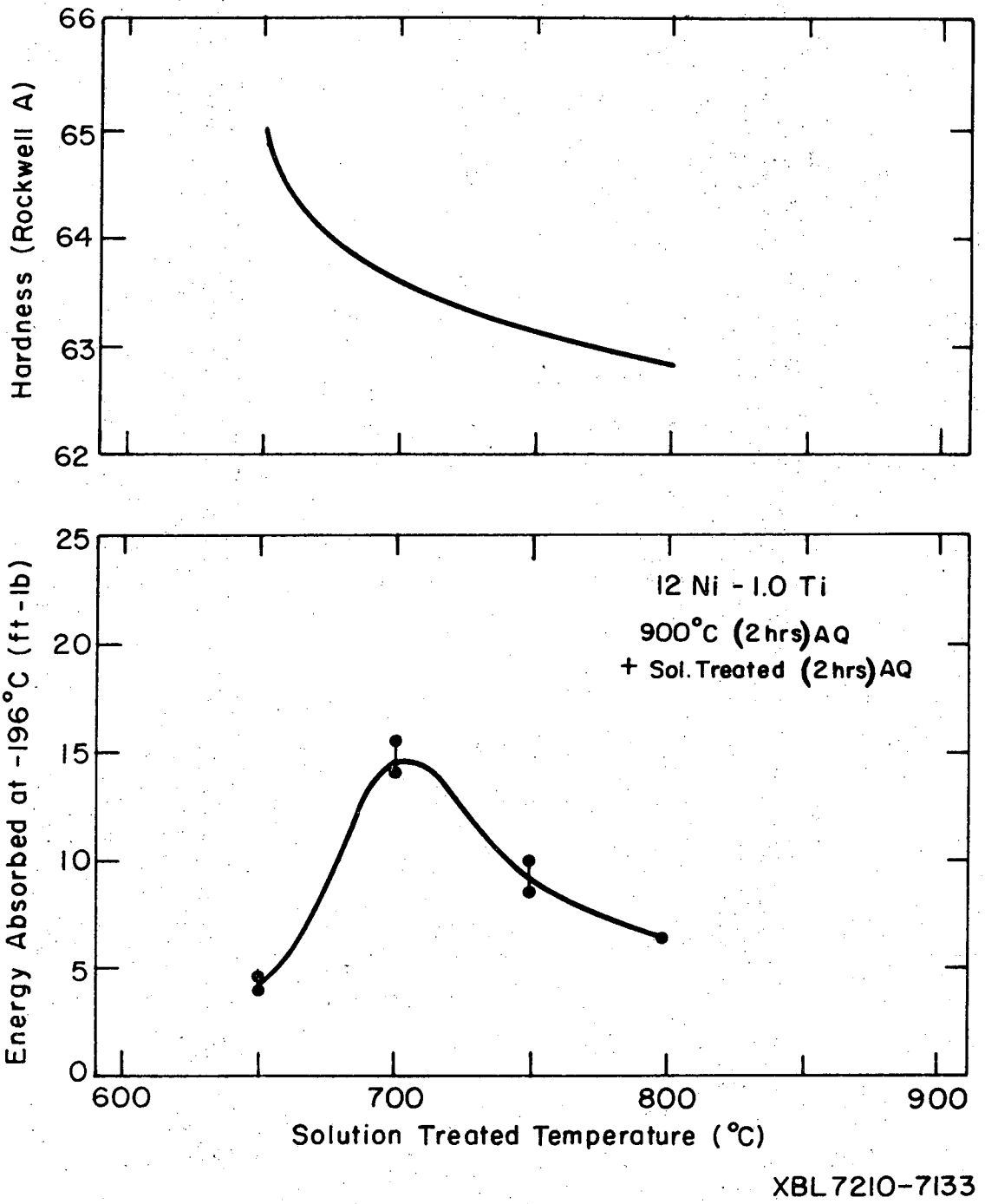

Charpy impact energy at -196°C and hardness vs temperature + AQ from the 900°C (2 hrs) AQ condition. Alloy: Fe-12 wt% Ni-1.0 wt% Ti.

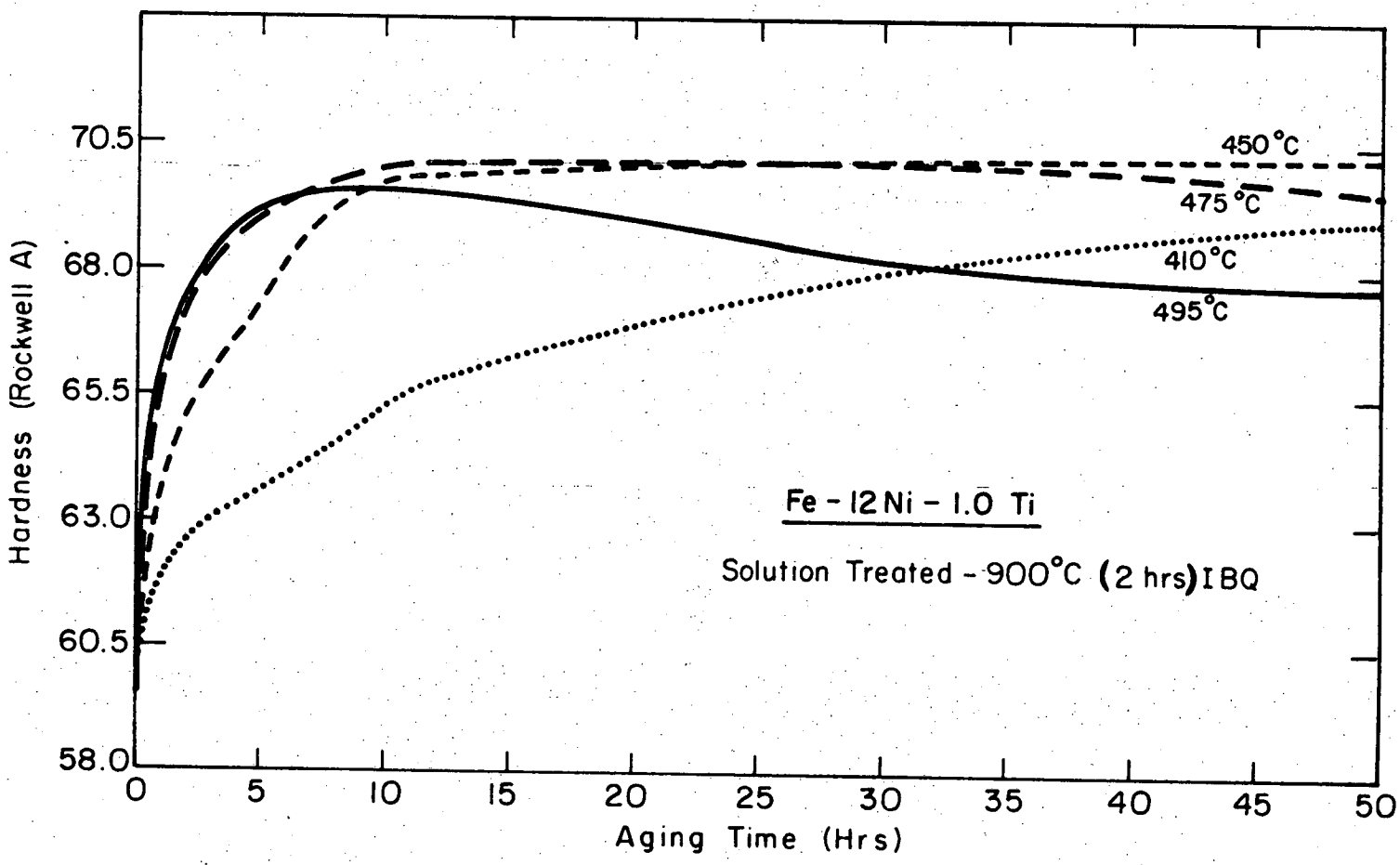

XBL729-6980

Hardness vs isothermal aging time of four temperatures from the 900°C (2 hrs) IBQ condition. Alloy: Fe-12 wt% Ni-1.0 wt% Ti.

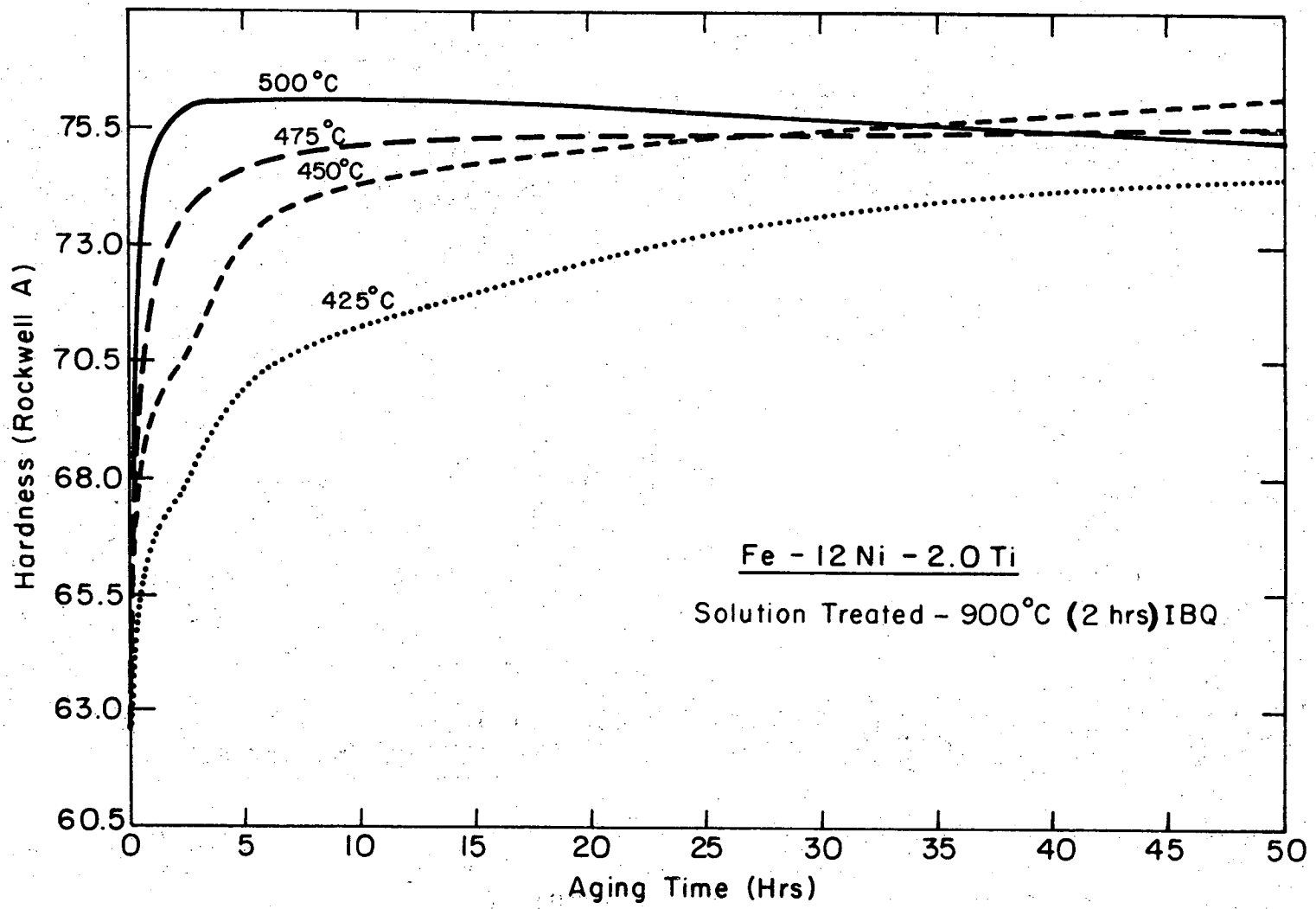

XBL729-6981

Hardness vs isothermal aging time of four temperatures from the 9-0°C (2 hrs) IBQ condition. Alloy: Fe-12 wt% Ni-2.0 wt% Ti.

Room temperature tensile data for 12 Ni, 1.0 and 2.0 Ti alloys in quench and precipitation hardened conditions.

		Heat Treatment			
		900°C (2 hrs) IBQ	900°C (2 hrs) IBQ + 450°C (24 hrs) BQ	900°C (2 hrs) IBQ + 475°C (22 hrs) BQ	900°C (2 hrs) IBQ + 600°C (0.5 hrs) BQ + 475°C (24 hrs) BQ
1.0 Ti	Tensile Strength (psi)	103,500	175,000		
	0.2% Yield Strength (psi)	97,000	169,500		
	% Elongation*	22.5%	21.0%		
	% Red. Area	82%	59%		
2.0 Ti	Tensile Strength (psi)	122,000		215,000	211,500
	0.2% Yield Strength (psi)	112,200			198,300
	% Elongation*	14.2%		0	10%
	% Red. Area	76%		0	33%

*1 inch by 0.25 inch diameter gauge length

TECHNICAL INFORMATION DIVISION
LAWRENCE BERKELEY LABORATORY
UNIVERSITY OF CALIFORNIA
BERKELEY, CALIFORNIA 94720